Soft Matter

Assembly and manipulation of responsive and flexible colloidal structures by magnetic and capillary interactions

Journal:	*Soft Matter*
Manuscript ID	SM-REV-01-2023-000090.R1
Article Type:	Review Article
Date Submitted by the Author:	26-Feb-2023
Complete List of Authors:	Basu, Abhirup; North Carolina State University at Raleigh, Chemical Biomolecular Engineering Okello, Lilian; North Carolina State University, Chemical and Biomolecular Engineering Morales Castellanos, Natasha; North Carolina State University at Raleigh, Chemical Biomolecular Engineering Roh, Sangchul; North Carolina State University at Raleigh, Chemical Biomolecular Engineering Velev, Orlin; North Carolina State University at Raleigh, Chemical Biomolecular Engineering

Soft Matter

Assembly and manipulation of responsive and flexible colloidal structures by magnetic and capillary interactions

Abhirup Basu,[#] Lilian Okello,[#] Natasha Castellanos, Sangchul Roh[$] and Orlin D. Velev*

Department of Chemical and Biomolecular Engineering, North Carolina State University, Raleigh, NC 27695, USA

[$] *Present address: Smith School of Chemical and Biomolecular Engineering, Cornell University, Ithaca, NY, 14853 USA*

[#] *Both authors contributed equally.*

* E-mail: odvelev@ncsu.edu

Abstract

The long-ranged interactions induced by magnetic fields and capillary forces in multiphasic fluid-particle systems facilitate the assembly of a rich variety of colloidal structures and materials. We review here the diverse structures assembled from isotropic and anisotropic particles by independently or jointly using magnetic and capillary interactions. The use of magnetic fields is one of the most efficient means of assembling and manipulating paramagnetic particles. By tuning the field strength and configuration or by changing the particle characteristics, the magnetic interactions, dynamics, and responsiveness of the assemblies can be precisely controlled. Concurrently, the capillary forces originating at the fluid-fluid interfaces can serve as means of reconfigurable binding in soft matter systems, such as Pickering emulsions, novel responsive capillary gels, and composites for 3D printing. We further discuss how magnetic forces can be used as an auxiliary parameter along with the capillary forces to assemble particles at fluid interfaces or in the bulk. Finally, we present examples how these interactions can be used jointly in magnetically responsive foams, gels, and pastes for 3D printing. The multiphasic particle gels for 3D printing open new opportunities for making of magnetically reconfigurable and “active” structures.

1. Introduction

The assembly of colloidal particles is generally categorized into two broad classes: self and directed assembly. Self-assembly can occur spontaneously due to intrinsic specific interactions in natural systems to form large scale structures such as lipid bilayers around live cells,[1] micelles from surfactants,[2] and DNA hybridization from complimentary strands of nucleotides.[3] However,

Soft Matter

most interactions on colloidal scale such as van der Waals, electrostatic and steric repulsion are unidirectional and lack specificity. Colloidal assemblies whose formation is driven by such conventional colloidal forces are commonly governed by minimization of interparticle interaction energy, or maximization of the entropy of the system.[4] One of the simplest approaches to colloidal assembly is the restriction of the volume, or drying of the suspensions, typically leading to the formation of isotropic closed packed 2D or 3D crystals.[5–8] Such assembly processes have been a focus of research interest as, for example, they allow to model some of the fundamentals in the atomistic level crystallization and defect formation. However, they are limited in their ability to form complex directionally oriented structures.[9]

Directional colloidal assembly techniques using external fields such as magnetic fields,[10–13] electric fields[14–17] and light[18,19] offer efficient ways of overriding the common colloidal interactions and guiding the particles to form out-of-equilibrium structures by accelerating the assembly kinetics. Further, external fields offer more precise control of the dynamics of the assembly process by changing the field parameters and can be used to assemble structures ranging from oriented 2D crystals,[20] nanowires,[21] electro and magnetorheological fluids to other stimuli responsive materials.[22] By tuning the field parameters, researchers are able to form multiple structural patterns that can be re-configured on-demand.[9,23,24] Additional complexity and directionality of the assemblies can be achieved by using patchy and shaped colloidal particles which are anisotropic in geometry, polarizability, or surface properties.[25–27]

The goal of this review is to summarize the rich variety of ways in which the field-driven assembly can be combined with multiphasic systems and capillary forces to form numerous classes of flexible responsive soft matter. The topics that are reviewed are schematically presented in **Figure 1**. First, we briefly introduce the fundamentals of magnetic interactions between isotropic colloidal particles, and the principles of magnetic field-directed assembly of structures in multiple dimensions (Figure 1a). This assembly is a convenient tool for making directionally responsive structures where the particles form large-scale hierarchical structures ranging from chains to sheets, to bundles and clusters (**Figure 1 a, b**). The magnetic field guided structuring is robust, rapid and is initiated and controlled outside the system without interfering with experimental parameters such as temperature, pH and solvent composition.[28–30] We discuss how multiaxial fields such as biaxial (rotating) or triaxial (precessing) ones introduce extra control parameters, which enable the assembly of a wide variety of complex morphologies.[31,32] Next, we extend these principles to probe into the recent advancements made in the assembly of magnetically reconfigurable structures using anisotropic or patchy particles (Figure 1b).

Soft Matter

The second group of topics in this perspective is how capillary forces provide another convenient set of techniques to control and manipulate particle structures. Colloidal particles adsorbed or protruding through fluid-fluid interfaces (liquid-air, or liquid-liquid) can experience capillary forces due to the deformation of the interface around them.[33–35] These forces are characterized by very long range and directionality, and can be attractive or repulsive depending on the shape of the meniscus between the particles. Alternatively, small amount of liquid can result in capillary bridging between particles and completely change the rheological properties of the suspension (**Figure 1c**). We further discuss how capillary interactions on the colloidal scale can be used in conjunction with magnetic fields to restructure various multiphasic colloidal systems,[36–40] resulting in magneto-capillary gels, foams and coatings (**Figure 1d**). A few classes of systems of specific interest include capillary pastes and gels for 3D printing (**Figure 1e**), which we discuss separately due to their large importance and diversity of applications. We conclude with a summary of the opportunities and perspectives for further research that can be conducted in this area.

Soft Matter

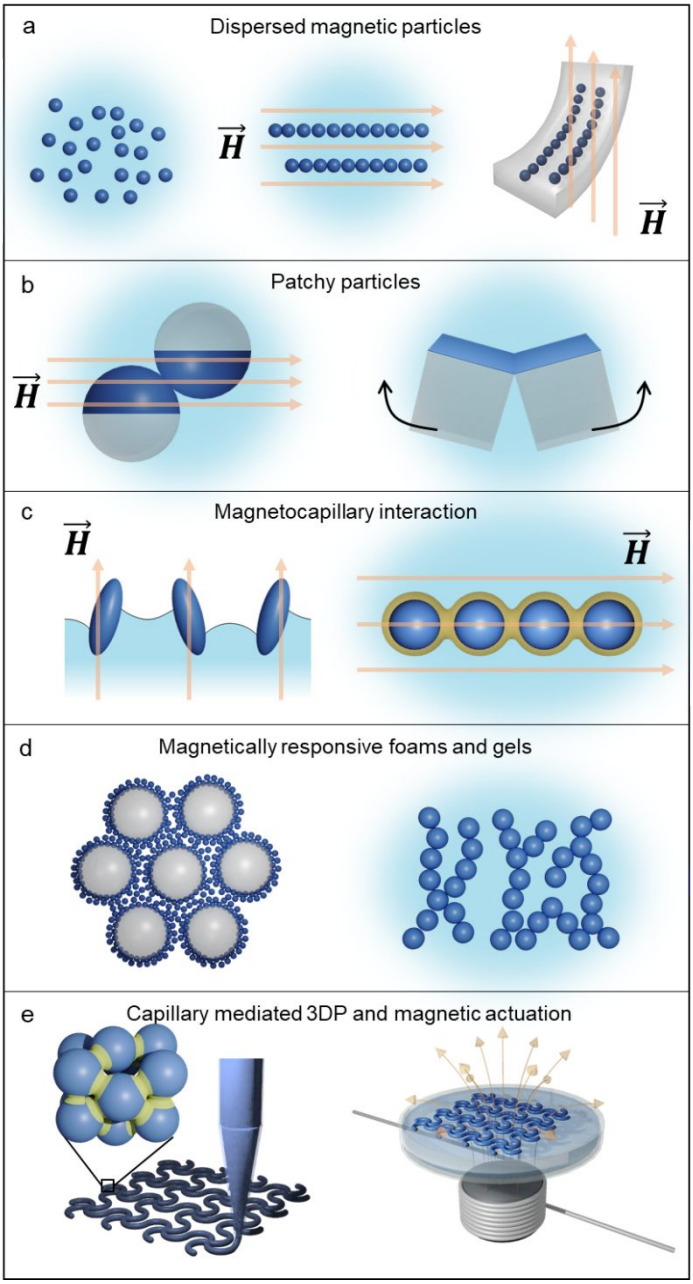

Figure 1: Highlights of the perspective review: **a)** Magnetic field guided assembly of isotropic colloidal particles dispersed in a liquid medium or embedded in a polymer matrix; **b)** Responsive structures assembled by anisotropic or "patchy" particles, for example, Janus spheres (left) and one-sided metal coated patchy microcubes (right); **c)** Interactions guided by magnetic field in conjunction with capillarity at interfaces (left) and in the bulk (right); **d)** Assembly of magnetically responsive foams (left) and gels (right); **e)** Capillary-mediated 3D printing (left) and magnetic actuation of soft matter (right).

Soft Matter

2. Assembly of colloidal particles via magnetic interactions

The availability of efficient means to generate magnetic fields in space and time has enabled a broad range of scientific investigations of the directed magnetic assembly of colloidal structures. Magnetic field induce polarization in the colloidal particles the extent of which is dependent on the orientation of the magnetic moments inside the material domains. In short, magnetic materials are classified broadly into three types: i) Paramagnetic, which have randomly oriented magnetic moments and align themselves along the field, but lose their magnetism upon removal of the field, ii) Diamagnetic where the atoms have no magnetic moments and are weakly repelled by an applied magnetic field, iii) Ferromagnetic, which are analogous to paramagnetic ones but contain permanently aligned magnetic moments and retain residual magnetization after the field is switched off. Amongst the various types of magnetic particles, superparamagnetic particles, mostly found in the size range of 3-50 nm are widely used for field-directed assembly because of their high magnetic susceptibility. Since each superparamagnetic particle contains a single magnetic domain, the polarized particles can be approximated as a point dipole. The interaction potential when the interparticle separation is much larger than the particle diameter (**Figure 2a**) between two dipoles $\overrightarrow{\mu_1}$ and $\overrightarrow{\mu_2}$ separated by a distance of r_{12} is given by

$$U_{12} = \frac{1}{{r_{12}}^3}[\overrightarrow{\mu_1}.\overrightarrow{\mu_2} - 3\frac{(\overrightarrow{\mu_1}.\overrightarrow{r_{12}})(\overrightarrow{\mu_2}.\overrightarrow{r_{12}})}{{r_{12}}^2}] \quad (1).$$

The simplest way of structuring such colloidal particles is the application of a static magnetic field, which aligns the particles along the direction of their magnetic moments. The magnetically polarized particles attract or repel each other depending on the mutual orientation of their dipoles. For two identical dipoles, the above equation can be simplified to

$$U_{12} = \frac{\mu^2}{{r_{12}}^3}[1 - 3cos^2\theta] \quad (2).$$

The attractive dipolar interaction is maximal when the particles are aligned in a "head to tail" configuration, i.e., $\theta = 0°$ (**Figure 2a**). Provided that the interparticle potential is strong enough to overcome thermal fluctuations, this leads to the formation of 1D linear chains, which represent the simplest hierarchy of the directed assembly. With the increase in angle between the particles, this attractive force decreases and vanishes at a "magic" angle of 54.7°, above which the particles encounter a repulsive force.[29,41] The rate of chain assembly is further dependent on the particle volume fraction and the effective capture radius, which is defined as the threshold interparticle distance at which the attractive potential is equal to the thermal energy kT.[42] Particles at greater distances apart rely on diffusion to enter into the capture radius. **Figure 2b** shows

snapshots of the aggregation of superparamagnetic polystyrene particles from a Brownian fluid system after applying a uniaxial magnetic field for 3000 s.[43] The cluster growth rate was found to vary monotonically with the particle packing fractions and magnetic field strength. The cluster size length followed a scaling relationship of $< L > = f\left(\emptyset^{\frac{5}{2}} B^2 t\right)$ where <L> defines the mean cluster size length, and ø, B and t represent packing fraction, field strength and time of application of magnetic field, respectively. The assemblies from superparamagnetic particles can disassemble or break apart upon removal of the field owing to their negligible residual magnetization. These assemblies and their field responsiveness can be preserved by embedding them inside soft polymer matrix[44–46] or physically or chemically binding the nanoparticles into flexible structures,[47–49] which will be discussed in the next sections.

The linear chains from magnetic colloidal particles can also coalesce laterally and form thick fibers (bundles) or crosslinked networked structures.[50,51] By calculating the interaction energy between lateral chains, Furst and Gast predicted that at shorter separation between two chains there exists either a repulsive or attractive potential depending on their mutual alignment.[51] The potential will be attractive if the chains are out of registry, and will be repulsive if the chains are in registry. As the field strength is increased, two chains can interact laterally at a critical field strength to overcome the energy barrier for lateral aggregation.[52] After coalescing laterally, the overall energy of the system drops, and the aggregation into bundles gets repeated at the next critical field strength (**Figure 2c**). One can observe further complex and structurally different network formation by applying more complex field configurations. For instance, linear networked structures comprised of T-, L- and "criss-cross" junctions can be assembled from paramagnetic colloidal particles by using alternating current (AC) and direct current (DC) magnetic fields orthogonal to each other (**Figure 2d**).[53] Further, disc-like clusters can be formed at the network junctions by increasing the frequency of the oscillating field,.

Paramagnetic colloidal particles can also condense into crystalline structures in pulsating magnetic fields.[54,55] Swan et al. studied the depercolation and crystallization of polystyrene latex beads with embedded iron oxide magnetic nanoparticles under toggled magnetic fields as a function of the frequency and applied field strength. They showed that a uniform pulsed field could be used to organize the disordered suspension into entangled chains (**Figure 2e**). While operating at frequencies lower than the relaxation time of the suspensions, the structures lost their "memory" at every pulse and reorganized themselves. However, at higher frequencies, the field-off portion of the pulse was so short that the assemblies could not overcome the kinetic constraints typical of strong dipolar interactions and self-assembled to condensed crystalline domains. Other condensed

Soft Matter

phases including close-packed hexagonal, square, labyrinth and honeycomb phases can be observed experimentally by using soft-core repulsive magnetic colloidal particles in presence of a transverse magnetic field,[56] in agreement with simulation results by other research groups.[57,58] Their spatial arrangement can be conveniently tuned by varying the particle density.

Complex hierarchical structures can be formed with such longitudinal assemblies if the static field is replaced by time- and space-varying magnetic fields, one of the simplest of which is the rotating magnetic field.[47,59,60] Magnetic and viscous forces are the two major factors governing this assembly dynamics in such fields. Earlier simulation studies showed that in contrast to the uniaxial fields, which drive the formation of chain-like structures, rotating fields could induce the organization of polarizable particles into sheet-like structures.[61–63] In reality, the chains undergo steady rotation at low field frequencies due to the magnetic torque, while viscous forces prevent their complete alignment and lead to the rotation of the chains with a phase lag angle. The phase lag angle increases with the increase of the length of the chains, which may result in their fragmentation.[64,65]

Further complexity can be introduced by precessing fields combining a static magnetic field around a particular axis (for example z-axis) with an orthogonal rotating magnetic field (x-y plane). In the presence of a precessing rotating magnetic field, the linear chains can buckle and transform into various configurations such as a dynamic helix, hairpin, S-shaped chain or others.[66,67] The chains can further break up at multiple points depending on the field rotation rate and can collapse into two-dimensional clusters in the case of very high-frequency rotating fields.[68,69] Hilou et al. observed the phase transition of a homogenous colloidal suspension to a bicontinuous phase and the formation of spinoidal microstates in the time-varying fields (**Figure 2f**).[70] While the clusters are loosely packed with no ordered structures at low field strength, they can finally form colloidal crystals with hexagonal ordering with increase in field strength (**Figure 2g**).[69] Osterman et al. predicted that this cluster formation is achieved due to long-range attractive potential between the particles in a precessing field.[32] Conversely, isotropic repulsive potential can also help in achieving ordered crystals with large interparticle spacings as compared to the crystals formed with attractive dipolar interactions. Thus, the magnetic interactions enable assembly on many length scales.

Soft Matter

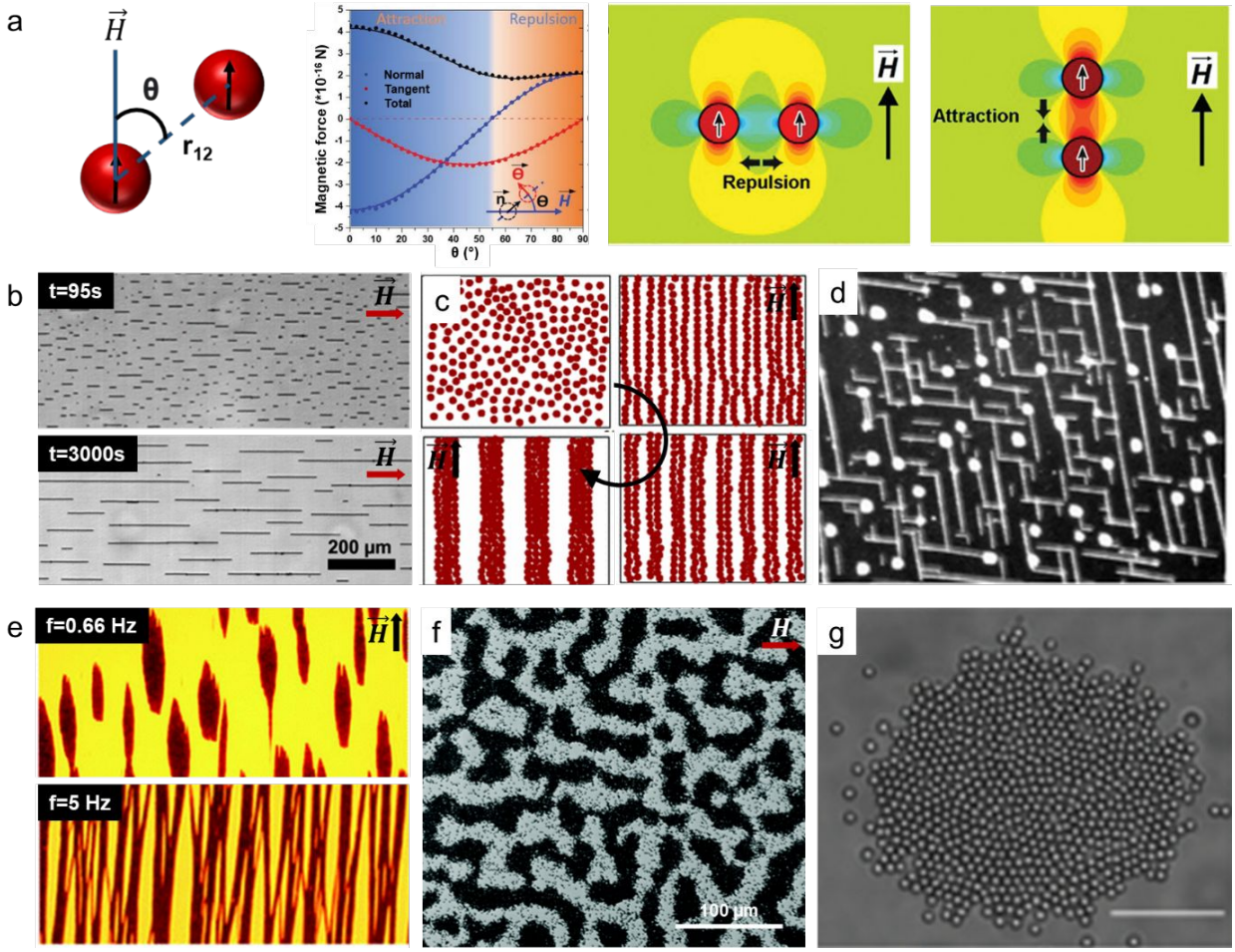

Figure 2: a) Schematic of the dipole-dipole interaction between two superparamagnetic colloidal particles and the corresponding total magnetic force with tangential and normal components as a function of the angle between them. It also shows the two limiting cases of magnetic interaction when the particles are oriented at 90° (side by side) and 0° (head-to-tail). Reproduced with permission from refs. [24,29]. Copyright 2020, Wiley-VCH and 2013, Elsevier. **b)** Optical snapshots of superparamagnetic colloidal particles forming linear chains and their growth in the presence of a uniaxial static magnetic field. Reproduced with permission from ref. [43]. Copyright 2015, American Institute of Physics. **c)** Lateral zipping of chains to form thick bundles in magnetic nanofluids under external magnetic fields. The arrow represents the increase in critical magnetic fields. Reproduced with permission from ref. [52]. Copyright 2009, American Physical Society. **d)** A network of linear structures with T-, L-, and "criss-cross" junctions under combined AC/DC magnetic fields. Reproduced with permission from ref. [53]. Copyright 2011, American Chemical Society. **e)** Magnetic field induced assembly into condensed (top) or percolated (bottom) structures from paramagnetic colloidal particles after applying pulsed magnetic fields at different frequencies. Reproduced with permission from ref. [55]. Copyright 2014, Royal Society of Chemistry. **f)** Phase separation

Soft Matter

followed by aggregation of paramagnetic particles into spinoidals after applying a high frequency rotational magnetic field. Reproduced with permission from ref. [70]. Copyright 2020, Royal Society of Chemistry. **g)** Optical micrograph of packed cluster with hexagonal ordering of paramagnetic carboxyl-coated polystyrene particles in a high frequency rotating magnetic field. Reproduced with permission from ref. [69]. Copyright 2018, American Physical Society.

3. Magnetic interactions and structures from anisotropic colloidal particles

Anisotropic colloidal particles are rapidly emerging topic of colloidal and materials research, partially due to the large diversity of structures that can be synthesized through their directed assembly. The anisotropy can originate from particle shape but can also be a result of surface modification.[71–74] In order to incorporate shape or surface anisotropy, numerous microfabrication techniques including photolithography, soft lithography, microfluidics and micromolding have been used to form patches of dissimilar charges, polarizability, or different functional groups attached to the particle surface.[75–80] The simplest class of such particles are hemispherically different "Janus microspheres", which have been fabricated and investigated widely in the assembly of hierarchical structures for both fundamental and industrial applications.[14,81,82] Many of the originally produced Janus particles have a metallic coating on one hemisphere of a polystyrene particle and a dielectric part on the other hemisphere and can vary in size from 100 nm to millimiters.[83,84] An anisotropic magnetic component can be introduced by metal vapor deposition of a thin magnetic film on the particle surface. Alternatively, magnetic nanoparticles can be attached to a portion of non-magnetic patchy particle by selective adsorption, taking advantage of the particle's differentiated surface properties.[85]

Upon switching on the magnetic field, the randomly oriented metallo-dielectric Janus particles can be assembled into "staggered" chains, aligned along the direction of the magnetic field. The orientation of the particles in the chains is guided by the strong interaction between the polarized metallic halves. The alignment of the dipoles in the metal leads to the staggered packing with the metal halves facing each other in alternate directions (**Figure 3a**).[10,86] The disassembly kinetics of these chains after switching off the magnetic field depend on the attraction of the neighboring particle by residual magnetic polarization, which in turn is a function of the thickness of the deposited metallic layer. For example, chains of "Janus" particles with a coating thickness of 8 nm came apart easily by small shear forces; while those with a coating thickness of 34 nm maintained their structures and could be disassembled only after demagnetization. Further, replacing the uniaxial field with other fields completely changes the assembly configuration. In particular, the "Janus" particles self-organized to produce hexagonal crystals under a rotating field

Soft Matter

of moderate strength with the metal coating pointing perpendicular to the plane of the field.[31] The constituent particles were found to rotate synchronously with the field. An increase in the field strength in this system formed new structures where the magnetic hemispheres of "Janus" particle pairs faced each other to form dumbbell-like clusters (**Figure 3a middle**).[87] Another time-dependent configuration using a precessing field causes the Janus particles to assemble into microtubules,[88] and stack as polygons (**Figure 3a right**). These particles also rotated in place but maintained the overall orientation and the structural integrity of the microtubes.

The use of shape-anisotropic particles also leads to the formation of chains and arrays of unusual symmetries. The localized dipole interactions and torque acting on the particles determine their orientation when the field is applied during the assembly process. Particle anisotropy also brings additional steric components, which directs the symmetry of assemblies and is also governed by the size and shape of the patches.[89,90] For example, doublets of two differently sized silica particles with a magnetic cap self-assemble into helical structures as a result of steric hindrance induced by the size differences. Further, polymer microcubes with a metallic coating on one side[11,12,91] or microcylinders with a metallic coating on one half[79] form straight or staggered linear chains in static magnetic field (**Figure 3b**). Our group has shown that the magnetic patches of such particles acquired a dipole which led to cube chain assembly parallel to the applied magnetic field.[11] In essence, the metal coated face acts as a structural director for the microcube assembly, and the local orientation of particles in the chains depends on the mutual interactions between the metal patches. Two adjacent cubes in a sequence can form cis- or trans-configurations where the metallic side can be aligned side by side or top-to-tail, respectively. These configurations correspond to two minima of the potential energy landscape. After the removal of the magnetic field, the particles retain residual magnetization and interactions, so that the microcube chains demonstrate active dynamic rearrangement of the assembled chains into bundled or partially wrapped configurations. As a result, these microcube chains can stretch and contract reversibly by switching on and off the magnetic field. The repetitive opening and closing of small "microscallop" clusters of magnetic microcubes immersed in non-Newtonian fluid can be used for their directional active propulsion.[92] The ability of these soft robotic devices to reconfigure on-demand can find applications such as novel microrheometers, microswimmers or microbots for biological applications.[91]

Soft Matter

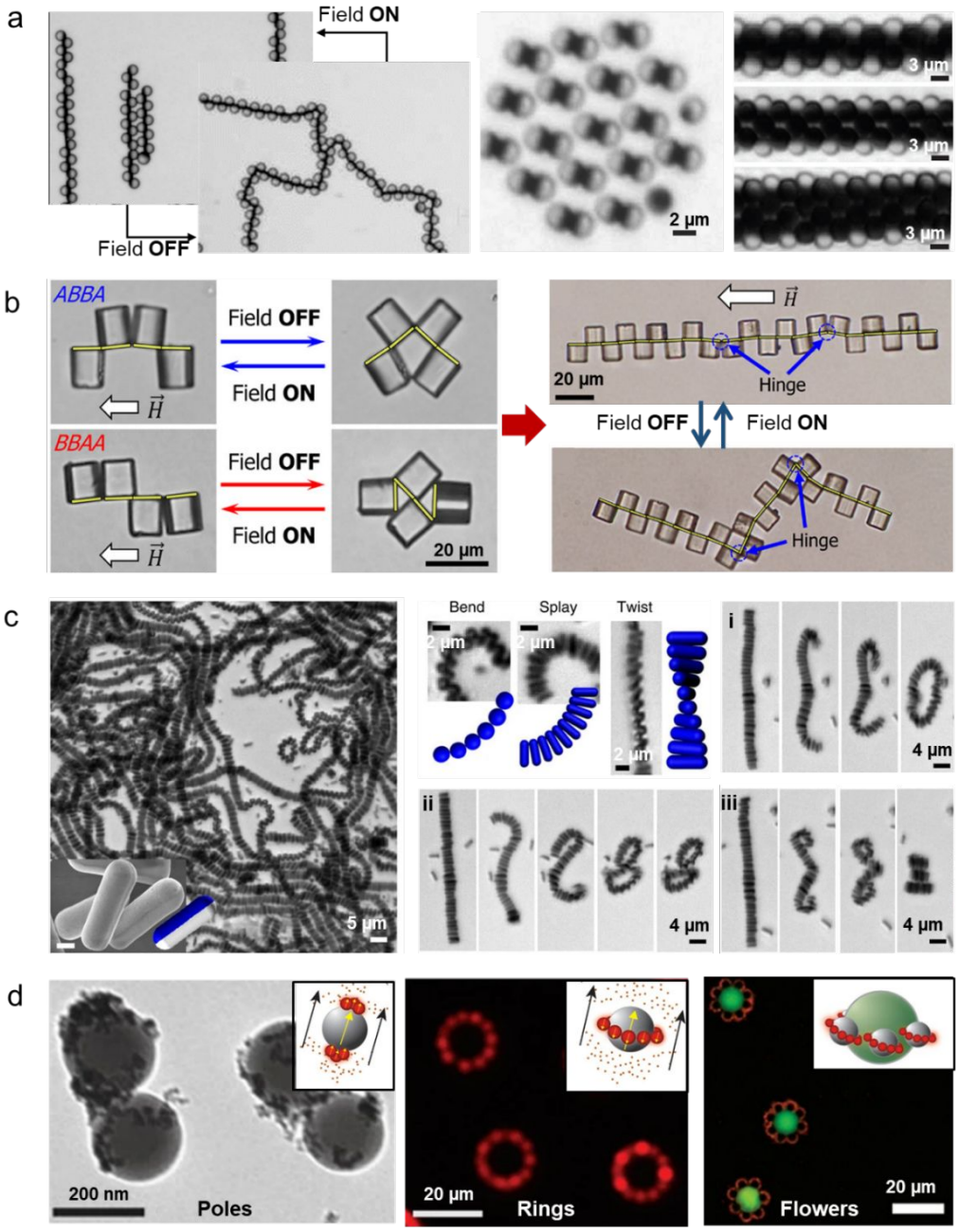

Figure 3: Reconfigurable structures guided by magnetic field: **a**) Linear double chains (left), dumbbell shaped dimers (middle) and microtubules (right) assembled from Janus spheres under the influence of uniaxial, rotating and precessing magnetic fields respectively. In the first case, the chains do not disassemble after switching off the field because of residual magnetization and may fold at various hinge points. Reproduced with permission from ref. [10,87,88]. Copyright 2009, Royal Society of Chemistry, 2014, Wiley-VCH and 2012, Nature. **b**) Patchy microcubes with a metallic coating on one side form two open configurations with the metal side facing each other or the metal side parallel to each other. The

Soft Matter

structures can reversibly open and close by toggling on and off the field. The cubes can form long linear chains in a concentrated system and can bend at suitable hinges upon switching off the field. Reproduced with permission from ref. [11]. Copyright 2017, AAAS. **c)** Optical micrograph of dipolar "Janus" rods forming colloidal ribbons (left) in uniform magnetic field. Modes of deformation of the ribbons and formation of cyclic structures upon reversing the direction of the field (right). Reproduced with permission from ref. [93]. Copyright 2013, Nature, **d**) Colloidal superstructures with multipole symmetry from diamagnetic (grey spheres) and paramagnetic (red spheres) particles in a magnetized ferrofluid medium (brown dots). Reproduced with permission from ref. [30]. Copyright 2009, Nature.

Other types of complex structures that have been reported use magnetostatic interactions of colloidal silica rods coated with a magnetic layer on one hemicylinder (**Figure 3c**).[93] These Janus rods were assembled into ribbons perpendicular to the applied field and were held in position even after field removal. These assemblies are also capable of undergoing deformations such as bending, buckling, and twisting and can be controllably reconfigured from ribbons to closed cyclic structures by reversing the direction of the field. The right panel of **Figure 3c** shows the evolution of rings by three major pathways where the ribbons either curve and the chain ends meet, or the ribbons split into fragments when the field reversal is very rapid. The ribbons could also stand vertically on a substrate in the presence of a relatively weak vertical magnetic field.

Finally, combining colloidal particles of unequal polarizability can also lead to the formation of various superstructures. Hierarchically assembled structures have been formed by applying a uniform field to a multicomponent suspension of diamagnetic and paramagnetic particles within a ferrofluid.[30] Here, the paramagnetic particles are attracted either towards the equator or towards the poles of the non-magnetic particles depending on the concentration of the ferrofluid, resulting in the formation of "rings" or "poles" (**Figure 3d**). In a 4-component system comprising of paramagnetic and two different sized non-magnetic particles in a ferrofluid, multipolar assemblies resembling axial octupoles ('flowers'), and mixed multipole arrangements ('two tone') have been observed. In another method, a ferrofluid suspension of patchy anisotropic particles with non-magnetic polystyrene particles showed that the latter particles aligned with the metallic core of the patchy particle diamagnetically.[13] Such assembly can be reversed on-demand by switching the field on and off, while permanent superstructures can be synthesized by replacing the surface coating of the non-magnetic particles with crosslinkable amino groups.

Soft Matter

4. Capillary mediated interaction and assembly

Capillary interactions present another powerful set of tools for assembling colloidal arrays and clusters. These interactions arise when colloidal particles partially wetted by liquid seek to minimize the energy of the liquid interface deformed around them.[94] Unlike smooth particles, surface roughness, defects, chemical composition variation, or other sources of pinned contact line in spheroidal and complex-shaped particles lead to complex undulated interface distortions.[33,95] Non-spherical particles can further create undulated contact line even in absence of rough surface or chemical composition variation.[96–99] Different classes of capillary phenomena resulting from such deformations were originally classified and analyzed in a series of seminal papers by Kralchevsky and coworkers.[100–102] The capillary interactions between particles are broadly classified into three classes illustrated in **Figure 4a**. In the first case, two particles floating on a liquid surface deform the flat interface due to gravity (**Figure 4a i**), acting against the interfacial tension of the liquid. This interfacial deformation makes the particles approach each other to reduce the overall interfacial and gravitational potential energies. While the particle weight plays the governing role in the origin of capillary forces between floating particles, the interaction can be driven by the wetting of the solid surface by the liquid as seen in the next two cases of particles confined in thin films (**Figure 4a ii and iii**). The interactions in this case are strongly affected by the magnitude of surface tension and the contact angle between the liquid and the particles. The former is called flotation forces, while the second one is called lateral immersion forces.[100,103] In the case of immersion forces, the particles are either restricted by a solid substrate at the bottom (**Figure 4a ii**) or confined in a thin liquid film joining the two particles (**Figure 4a iii**). The flotation force between two spherical particles of the same size is approximately proportional to r^6, while the immersion force is proportional to r^2, where r is the radius of the particle.[104] For floating particles, the competition between the thermal forces and the interfacial forces becomes prominent as we move from micron scale to nanoscale, leading to the instability of the assembled structures with nanoparticles because of thermal fluctuations.[105,106] However, in case of immersion forces, the thermal energy is usually lower than the interfacial energy by several orders of magnitude, so that both microparticles and nanoparticles confined on a solid surface can interact strongly. It is useful to note in this context that the capillary forces in thin wetting films are not the major origin of evaporative particle assembly as frequently assumed, as the latter is primarily driven by the convective transport of colloidal particles due to evaporation of water.[107,108]

Soft Matter

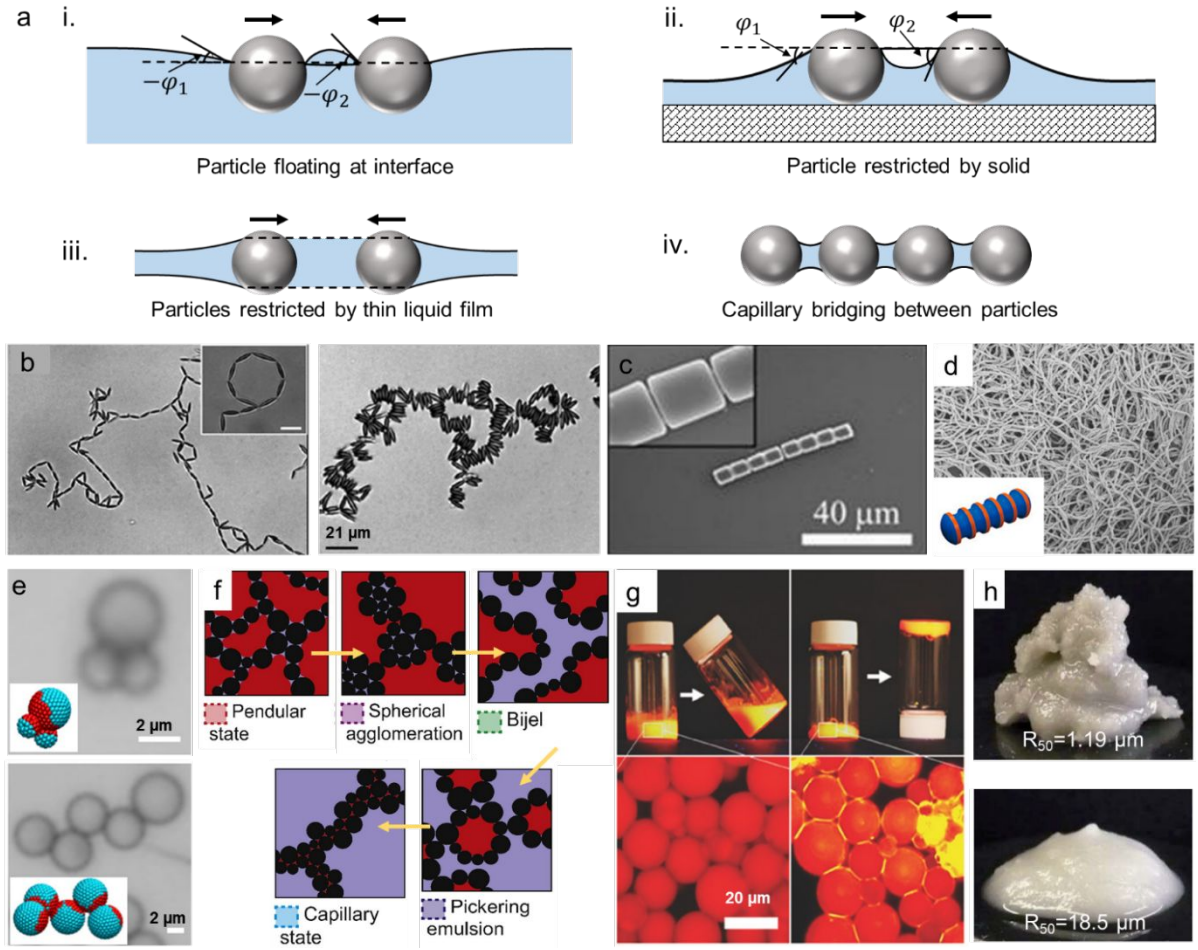

Figure 4: a) Schematic of the capillary interaction between two particles that are i) floating at fluid-fluid interface, ii) restricted by a solid surface from the bottom, iii) confined in a thin 2D liquid film, and iv) capillary bridging pulling them together. Capillary assembly of shaped anisotropic colloids: **b)** Polystyrene ellipsoids forming tip-to-tip and silica ellipsoids forming side-to-side configurations at oil-water interface. Reproduced with permission from ref. [113]. Copyright 2005, American Physical Society. **c)** Chains of SU-8 cylinders at an oil-water interface. Reproduced with permission from ref. [114]. Copyright 2010, American Chemical Society. Capillary assembly of patchy particles via capillary bridging: **d)** Long colloidal chains formed from polystyrene discs with two liquid patches. Reproduced with permission from ref. [115]. Copyright 2019, American Chemical Society. **e)** 3D and 2D architectures assembled from "Janus" microspheres (top) and double patched microspheres (down). Reproduced with permission from ref. [116]. Copyright 2016, American Chemical Society. **f)** Schematics of different particle-liquid-liquid systems with increasing volume fraction of preferentially wetting liquid. The two extremes, i.e., the pendular state and the capillary state represent capillary suspensions. Reproduced with permission from ref. [117]. Copyright 2014, Elsevier Ltd. **g)** "Homocomposite" capillary paste prepared from PDMS beads in liquid-like

Soft Matter

suspension (right), which gels after adding liquid PDMS precursor bridging the beads (right). Reproduced with permission from ref. [118]. Copyright 2017, Wiley-VCH. **h)** Effect of particle size on the rheological properties of capillary suspensions. Reproduced with permission from ref. [119]. Copyright 2012, Royal Society of Chemistry.

The flotation and immersion forces can be attractive or repulsive depending on the curvature of the liquid menisci, i.e., they are attractive when $sin\varphi_1\, sin\varphi_2 > 0$ and they are repulsive when $sin\varphi_1\, sin\varphi_2 < 0$. In addition to above-mentioned two types of capillary forces, there is a distinct third class of capillary "bridging forces", where the particles come into contact while bound by small volume of liquid (**Figure 4a iv**). Mechanistically, capillary bridging forces act normal to the line of contact of the particle surface, whereas the capillary flotation and immersion forces act tangential to the line of contact. Notable contributions by several research groups have enabled a broader understanding of the origin of capillary forces and have derived the analytical expressions of these forces,[109–112] which are outside the scope of the current review. Here, we will review some of the recent advances that have been made in capillary mediated assembly and their role in gelation and rheological processes.

The group of Whitesides was among the first to report the assembly via lateral capillary forces of millimeter and sub-micron scale objects into two dimensional arrays at the perfluorodecalin/water interface.[120,121] Capillary assembly of shape anisotropic colloids such as ellipsoids with different material properties has also been investigated.[34,113,122,123] At relatively small surface coverage, bare polystyrene ellipsoids at the water–oil interface have been observed to assemble tip-to-tip, while silica-coated polystyrene ellipsoids assembled side-to-side (**Figure 4b**). Surprisingly, as the solid fraction is increased, charged polystyrene ellipsoids change the assembly configuration at either the oil–water or air–water interface and form compact percolating networks with local dominance of triangular or flower-like structures.[123] By changing the particle shape from ellipsoids to cylinders, structurally different architectures such as end-to-end assemblies on planar interface at low particle concentration (**Figure 4c**) or "bamboo like" structures at higher particle concentration have been observed.[114,122]

Capillary bridging of patchy colloids also opens opportunities to form hierarchical structures. Solid patches are generally used, and liquid patches have been used in a few recent studies. Zhao et al. showed a simple method of forming 1D colloidal chains by capillary bridging.[115] Polystyrene discs with two liquid patches were centrifuged, during which the liquid patch of the discs compressed against each other and formed bridges binding the discs in a directional chain with parallel orientation (**Figure 4d inset**). The length of the chains increased

Soft Matter

with repeated cycles of centrifugation until they merged into long fibers without any external fields as exemplified in **Figure 4d**.

Higher ordered structures can also be made using capillary bridging. Our group used polystyrene microbeads with iron oxide patch on one hemisphere selectively wetted with liquid lipid fatty acids that can aggregate into three-dimensional clusters by directed capillary bridging.[116] By using different sized particles, we were able to observe biparticle dimers, trimers (**Figure 4e top**), hexamers and even particle rings. The cluster arrangement is guided by the balance between electrostatic repulsion and capillary bridging forces of the liquid phase of the fatty acids. Monte Carlo simulations showed how the assembly was affected by changing the patch areas. Further, by incorporating double patches on the particles, the arrangement hierarchy shifted from 3D to 2D clusters because of an additional directionality in the assembly that facilitated the formation of elongated structures (**Figure 4e bottom**). Disassembly of colloidal structures is also an important aspect that has been studied recently in applications which require high surface-to-volume ratio.[116,124,125] Interestingly, in the case of capillary mediated assembly, temperature-driven switching of these fatty acids from fluid to gel phases or swelling/deswelling of the patches around the particles is possible. In suitable solvents, this provides a variable that can be used to reversibly control the assembly/disassembly of the clusters.[116,126] Finally, capillary bridging can be combined with polymerization to construct complex permanent clusters.[127,128]

Capillary forces are efficient in the assembly of particles in that they can overcome repulsive electrostatic forces and are usually larger than van der Waals forces, giving rise to strong and cohesive colloidal structures. Even a small fraction of secondary liquid forming capillary bridges between particles could form percolated network in a concentrated multiphase suspension.[117,119,129,130] Capillary suspension can be formed with either the secondary fluid wetting the particles more favorably than the bulk phase, which is called the pendular state, or less favorably than the bulk, which is called the capillary state (**Figure 4f**). In both cases, the capillary suspension can transition from a viscous fluid to a gel-like material due to a meniscus particle bridging. This can result in dramatic changes to the rheological properties of a suspension.[131–134] It has been shown that increase in the wetting liquid's volume fraction also results in states without percolated network formation, such as Pickering emulsions, Bijels or spherical agglomerates.

Capillary force offers strong yet controlled binding and aggregation in a liquid medium. Capillary force-mediated gelation has also been studied by Hoffman et al. to establish how particle size affects the rheology of suspensions and gels, as quantified by their yield stress and shear viscosity.[119,134] To quantify the capillary gel's strength versus particle size relationship, they prepared suspensions of hydrophilic glass microbeads with different sizes in liquid diisononyl

Soft Matter

phthalate (hydrophobic medium). While both samples immediately gelled due to strong capillary force interactions, the sample with larger glass beads formed a weak gel that sagged under its own weight (**Figure 4h**), inferring that the mechanical strength of the gel is inversely proportional to the radius of the constituent particles. Particle surface roughness was also found to influence the rheology of capillary suspensions, as weaker and less clustered structures were formed when increasing particle roughness.[135] Such ability to tune the material properties is specifically useful when making capillary pastes for applications such as extrusion-based 3D printing.[136–138] The resulting structures can be made reconfigurable by modifying parameters such as temperature, wetting liquid properties, and the three-phase contact angle. Our group presented a simple universal technique for making "homocomposite" capillary pastes for 3D printing.[118] It uses the same common silicone base (polydimethylsiloxane, PDMS) for making elastomeric particles as well as the liquid capillary binder phase. We prepared dispersions of PDMS microbeads by emulsion polymerization. These beads were gelled by capillary bridging action after uncured PDMS liquid precursor is added to the suspension (**Figure 4g**). The result is a capillary paste with yield stress that can be conveniently extruded by 3D printing as discussed in Section 7

5. Assembly at fluid-fluid interfaces using magneto-capillary interactions

The synergistic combination of easy to control magnetic actuation and long-range reconfigurable capillary interactions allows to construct a variety of structures with remarkable properties and dynamic responses. Time-varying magnetic fields could be applied to form reconfigurable out-of-equilibrium particle patterns at interfaces. Millimeter size-discs deposited on the water surface can spin in place with an angular speed equal to that of the applied rotating magnetic field from the bottom.[139] Disc spinning was found to generate hydrodynamic forces which induced repulsive interactions, while the discs were simultaneously attracted towards the axis of the rotating field. This interplay between these competing forces led to the formation of dynamic assemblies with unusual ordering. An in-plane rotating magnetic field operating at a frequency of 1 Hz in conjunction with a vertical uniform magnetic field can lead to collection of metallic spheres suspended at the air-water surface rotating jointly at an angular speed of 0.3 rad s^{-1} **(Figure 5a).**[140] The rotational speed was found to be dependent on both frequency and strength of the field. The authors suggest that such non-reciprocal motion can be used for the design of microswimmers.

Soft Matter

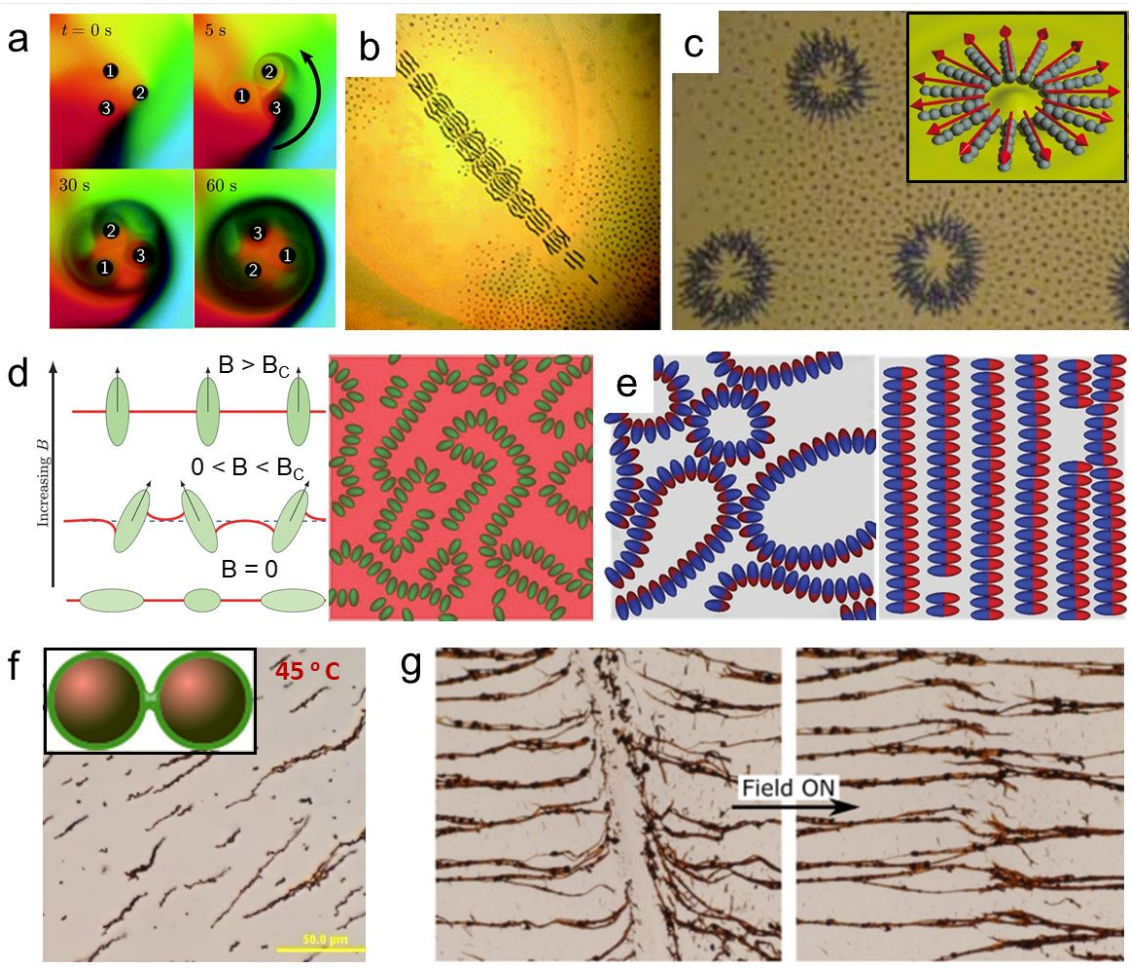

Figure 5: Magneto-capillary assembly of colloidal particles: **a)** Locomotion of a capillary assembly of 500 µm magnetic spherical particles exposed to vertical and a horizontal rotating fields. Reproduced with permission from ref. [140]. Copyright 2019, Royal Society of Chemistry. **b)** Self-assembled "snake" like patterns with multiple segments generated by an AC magnetic field at an air-water interface. Reproduced with permission from ref. [37]. Copyright 2006, American Physical Society **c)** Self-assembled dynamic asters at the liquid-liquid interface (left) and schematics of a magnetic ordering in asters (right). Reproduced with permission from ref. [36]. Copyright 2011, Nature. **d)** Schematic of the alignment of ellipsoidal magnetic particles with increasing field (left) and formation of "capillary caterpillars" of ellipsoidal particles in side-by-side configuration at air-liquid interface (right). Reproduced with permission from ref. [38]. Copyright 2014, Wiley-VCH. **e**) Magnetic assembly of ellipsoidal "Janus" particles into structures such as rings, chains, and hexagonal lattices. Reproduced with permission from ref. [145]. Copyright 2021, Wiley-VCH. **f)** Permanent flexible filaments magnetically assembled by Fe_2O_3 nanoparticles bound by liquid fatty acid. The inset shows the schematic of liquid nanocapillary bridging between the nanoparticles. Reproduced with permission from ref. [39]. Copyright 2015, Nature. **g)** Self-repairing capability of the microfilaments

Soft Matter

where the broken filaments reconnect with each other after applying magnetic field. Reproduced with permission from ref. [39]. Copyright 2015, Nature.

Magnetic colloidal dispersions can also assemble in unique patterns at fluid interfaces by applying an alternating magnetic field perpendicular to the air-water interface. A ferromagnetic dispersion can self-organize into "snake-like" structures illustrated in **Figure 5b.**[37,141,142] Each segment of these structures consists of ferromagnetically aligned microparticles, while the segments are antiferromagnetically oriented to each other. Pure magnetic interactions would make this configuration energetically unfavorable. Therefore, the authors attributed this pattern formation to the collective effect of magnetic dipolar interactions and induced hydrodynamic flows. The particles form aligned chains due to dipole-dipole interactions, while simultaneously dragging the surrounding fluid by their local oscillations at the interface. This combination leads to the formation of snake-like dissipative structures. Replacing the liquid-air interface with liquid-liquid interface can modify the outcome of such dynamic self-assembly and particles at an interface of two immiscible liquids exhibited the formation of localized asters (**Figure 5c**).[143] This dynamic self-assembly pattern is promoted by the interplay between the interface's excitations and a collective response of the magnetic colloids to the external alternating field.[144] Upon application of a small static in-plane magnetic field one can open-up and navigate the motile asters.

Davies et al. have investigated the behavior of shape-anisotropic (ellipsoidal) particles adsorbed at fluid-fluid interfaces under the influence of a magnetic field.[146] In absence of a magnetic field, the major axis of the ellipsoidal particles aligned along the interface without any surface deformation. When a magnetic field was applied normal to the interface, the magnetic torque tried to align the particles along the field. This caused menisci formation at the interfaces with depression on one side and elevation at the other and subsequent particle interactions. Monte Carlo simulation studies have also predicted similar discontinuous transitions and the critical field strength was found to be dependent on the particle size, aspect ratio and surface tension.[147,148] In a concentrated system, the ellipsoids assemble in "capillary caterpillars", and various configurations where particles align side-to-side (**Figure 5d**).[38]

Xie et al. also investigated the interaction of Janus ellipsoidal particles adsorbed at fluid-fluid interface.[145] These particles are composed of polar and apolar halves of opposite wettability. By applying orthogonal uniaxial fields, the tilt angle of the Janus ellipsoids with respect to the interface can be tuned, which ultimately leads to the formation of various ordered structures such as clusters, chains, hexagonal lattices, and ring-like structures, as predicted from the simulation results (**Figure 5e**). Similar simulation studies have been done by Xie et al. on the interface

Soft Matter

deformation by Janus particles adsorbed at fluid-fluid interfaces under the influence of a homogenous magnetic field.[149] Lattice-Boltzmann simulations predicted dipolar deformation of the interface, which increased linearly for smaller tilt angles and reached a constant value for higher tilt angles till 90°. Using this fundamental interpretation of dipolar capillary interactions of Janus particles at the interfaces, they further developed a pair-interaction model that predicted that these particles would arrange into a side–side configuration in a concentrated system and form monolayer structures. The particles arranged into long, straight chains, in contrast to the structures formed by capillary interactions between ellipsoidal particles.[150]

Magneto-capillary forces in the bulk of liquid phases can also be used to form flexible particle chains and networks. One such example is the magnetic assembly of Fe_2O_3 nanoparticles surrounded by a surface-condensed liquid lipid layer.[39,151] Our group demonstrated that under the influence of a uniform magnetic field, the lipid-bound nanoparticles formed microfilaments, which have extremely high flexibility due to the lipid capillary bridges between the nanoparticles (**Figure 5f**). The capillary bridges were able to reform and self-repair by reconnecting the broken filaments when the magnetic field was re-applied (**Figure 5g).** The filaments were fully stretched under constant magnetic field and tried to follow the field direction. Once complex fields such as rotating magnetic ones were introduced, the filaments curled, stretched, bent, and bundled, giving rise to a variety of unusual shapes such as closed rings, or closed infinity signs. Similar principles for capillary binding of magnetically responsive structures were used in the formation of 3D printable pastes described in Section 7.

6. Magnetically responsive foams, gels, and coatings

Various combinations of magnetic and capillary forces can be encountered in many classes of multiphasic systems of practical importance, including foams, emulsions, gels, and coatings. We review below recent advances in such areas leading to novel responsive and reconfigurable systems.

Foams. Pickering stabilization of foams by adding solid particles to the dispersion has been established for long; but only relatively recently researchers have shown how the Pickering foam stability can be manipulated using external fields. One simple way to make field-responsive foams is the introduction of the inorganic magnetically responsive particles to foams which can stabilize the foams and allow their manipulation by an external magnetic field.[152–155] Similarly, Pickering emulsions containing paramagnetic particles can be reversibly switched between biphasic dispersions and fully phase-separated fluids upon application of a magnetic field.[60,156]

Soft Matter

Magnetically responsive particles can also be used to tune the shape and stabilities of the bubbles in the foams using an external magnetic field.[156–160] Soetanto and Watarai showed the motion control of 10 μm sized bubbles stabilized by submicron magnetite particles. The magnetic particles functioned as both the force mediator and the bubble stabilizer. Magnetic fields can be used to twist the structures and tune the size of the bubbles in ferrofluid foams[161] and other magnetically responsive foams stabilized by hydrophobic magnetic nanoparticles.[156]

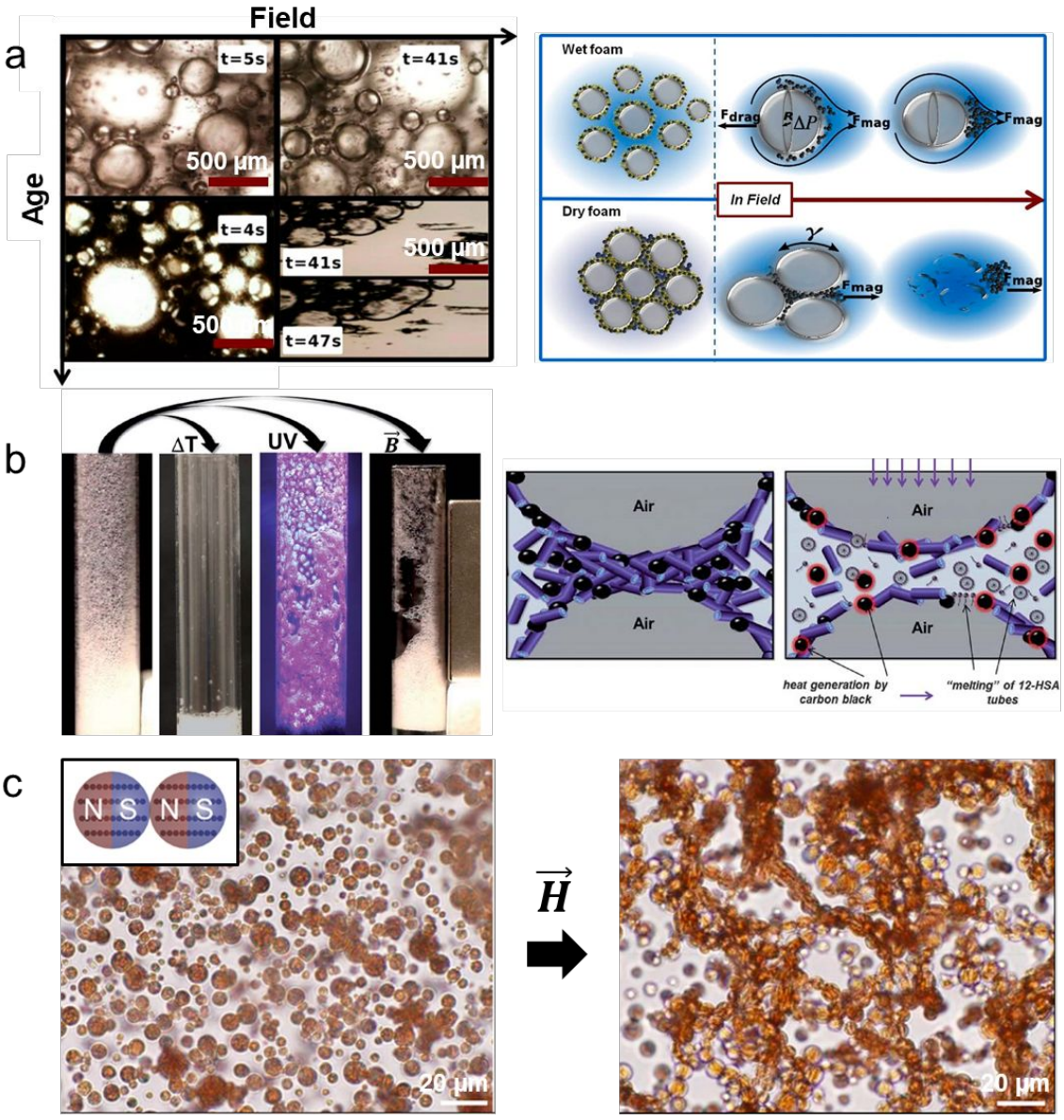

Figure 6: a) Magneto-Pickering foams stabilized by hypromellose phthalate particles with embedded carbonyl iron particles. Optical images of collapse of wet foam (top) and dry foam (bottom) and a

Soft Matter

schematic of their corresponding destabilization mechanisms in magnetic fields. Wet foam collapses due to ejection of bubbles from the foam matrix, while the dry foam collapse occurs due to film breakup and bubble coalescence. Reproduced with permission from ref. [162]. Copyright 2013, American Chemical Society. **b)** Foams prepared using 12-hydroxystearic acid containing magnetic particles destabilized by multiple stimuli including increase in temperature, UV irradiation and magnetic field exposure (left). Schematic illustrating the collapse of the foam after UV irradiation (right). Reproduced with permission from ref. [163]. Copyright 2013, Royal Society of Chemistry. **c)** Magneto-responsive gels derived using soft elastomeric PDMS microbeads with embedded chains of iron-oxide nanoparticles. After switching on the field, the dispersed beads aligned themselves along the field direction and formed percolated network-like structures. Reproduced with permission from ref. [164]. Copyright 2021, American Chemical Society.

The introduction of magnetic particles in Pickering foams also enables the formation of foam systems with on-demand breakdown and release as reported by Lam et al.[165] The foams containing hypromellose phthalate particles, with embedded carbonyl iron particles were stable for more than a week in the absence of magnetic fields but readily destabilized within seconds when a magnetic field above a certain strength was applied (**Figure 6a**). The breakdown of fresh foams was slow as the higher water content allowed for the migration of individual particles towards the field gradient, followed by the ejection of the air bubbles.[162] The liquid drainage from the films between the bubbles with aging led to thin, but fragile, films. These films are instantly broken by the magnetic particles when a field is applied, resulting in instantaneous foam collapse. Manipulation of Pickering emulsion can also be achieved by heating up the metal particles present in the foam matrix as shown by Kaiser et al.[166] Magnetic heating in the presence of an alternating field, can lead to complete miscibility of all components of the emulsion, which collapses the emulsion.

The next goal in this research area was to synthesize multi-field responsive soft materials based on foams. Fameau et al. reported the first multi-responsive foams with thermo-photo-magneto-controlled stability.[163] These foams were prepared by stabilizing the foams with carbon black particles (CBP) or and a thermo-responsive fatty acid, 12-hydroxystearic acid (12-HSA).[162,167] In the absence of UV irradiation, the 12-HAS forms tubular micelles, which jammed to form gel-like layers inside the foam films and trapped the CBP particles. CBP particles are intense light absorbers that in turn result in a rise in temperature, when exposed to UV light. The molecular 12-HAS assemblies transformed to micelles, thereby destabilizing the foam (**Figure 6b**). Thus, Fameau et al. were able to rapidly defoam systems containing magnetic carbonyl iron particles by either light, heat or by applying an external magnetic field.

Soft Matter

Gels: Magnetorheological gels (MRG) have also been a topic of investigations due to their potential applications in sensors, magnetoresistors, vibration control, brakes, mechanical dampers, and electromechanical devices.[168–171] Structurally, MRGs can be considered as an intermediate of magnetorheological fluids (MRFs) and magnetorheological elastomers (MREs). Gels are more liquid-like than the solid elastomers and allow for magnetic particle reconfiguration. Castellanos et al. reported magnetic-field induced gels composed of PDMS beads with embedded magnetically assembled and aligned chains of Fe_2O_3 nanoparticles (**Figure 6c**).[164] The formation of a percolated network between the microbeads made the system switch from fluid-like to gel-like structure upon turning on the field. These networks could be broken and reformed by cyclic demagnetization and remagnetization. Furthermore, as mentioned in the previous section, the combination of the magnetic and capillary interactions allows the formation of magnetically responsive capillary gels.[39] The dynamic response of such magnetic gels can be tuned by varying system parameters such as introducing an external field, varying the spatial magnetic particle distribution inside the polymer matrix, or the orientation memory of the particles.[172] Their magnetoresistance and elastic modulus could be further conveniently and reversibly adjusted by using magnetic fields.[170,173]

Lalitha et al. presented the design and synthesis of magnetically responsive self-healing gels composed of renewable resources.[171] They incorporated Fe_3O_4 nanoparticles into the gel matrix by sonication and demonstrated successful self-repair of these gels both in air and water medium. Other examples of biodegradable magnetic polymer gels are presented by Chatterjee et al., who used hydroxy-propyl cellulose and surfactant-modified maghemtie to synthesize a nanomagnetic gel using an emulsion method.[174,175] Akin to the multi-stimuli responsive foams, researchers have also aimed to investigate multiresponsive colloidal gels. For example, Braim et al. reported thermoresponsive magnetic colloidal gels composed of PDEGMA/poly(chloromethlystyrene) microspheres and Fe_3O_4 magnetic nanoparticles, which showed good cytocompatibility and could be used as 3D scaffolds for *in vitro* stimulation of cells.[176] Other types of thermoresponsive magnetic hydrogels and their applications are discussed in numerous reports.[177–179] Thus, both magnetic foams and gels are finding use in variety of fundamental studies and industrial applications.

One emerging application of comprehensive gel-based systems is in "slime robots," which represent a new class of magnetic robots based on liquid metal or ferrofluid.[180–183] Because of their fluid or gel-like characteristics, they exhibit better deformability than elastomer-based soft robots and can be guided to move and to pass through restricted spaces such as biological tissues. Sun et al. demonstrated one such fluid-based microrobot actuated by magnetic field, which can serve in

Soft Matter

various functions such as transportation, grasping objects, human motion monitoring, and circuit switching and repair.[173]

Coatings: Lee et al. presented a method of making coatings by utilizing the magnetic response of ferrofluid containing nonmagnetic colloidal particles.[184] Drying of droplets to deposit coatings from colloidal suspension leads to migration of the particles towards the edge of the droplets due to convective assembly, thereby forming coffee rings. The researchers showed how the coffee ring effect can be overcome by applying magnetic fields to a mixture of Fe_3O_4 nanoparticles and polystyrene latex beads. The direction of the particle motion towards the drying periphery was reversed as the field was switched on, causing them to move back from the edge and towards the center. This led to the formation of a particle-rich state at the center, with disc-like structures. This magnetostatic microconvection technique can be used in the deposition of functional coatings.

7. Responsive soft composites via magnetic and capillary interactions

The making of soft structures that can be reconfigured by external stimuli often requires the formation of lattices and networks of complex shape. 3D printing has emerged as an advanced fabrication tool for making soft reconfigurable structures due to its rapid prototyping capability. One of the most common methods for 3D printing of soft matter is direct ink writing (DIW) commonly based on extrusion of filaments through a nozzle. The gentle processing allows the extrusion of soft matter such as hydrogels[185,186] or elastomers.[187,188] The soft inks used for extrusion often contain particles or rheology modifiers to adjust yield stress and shear thinning, which allows extrusion at high shear stress followed by rapid solidification. *De facto*, the pastes used in 3D printing by extrusion are commonly a soft composite material on their own.

Common rheology modifiers that have been used to impart viscoelastic properties in extrudable pastes include fumed silica and clay particles. In addition to having the right rheological characteristics, the internal or external structure of extruded filaments can be engineered to include components that encode shape reconfiguration for applications such as soft actuators,[188–191] novel responsive gels,[28,163,192,193] biomedical applications,[194,195] and new drug delivery techniques.[196,197] One such example is biomimetic 4D (time-dependent) printing of hydrogel inks **(Figure 7a)**.[186] Cellulose fibrils could be used for internal structuring of the gels, where, after being shear-aligned during the ink extrusion, they can gave rise to their anisotropic swelling/deswelling and shape reconfiguration.[193,198–200]

Soft Matter

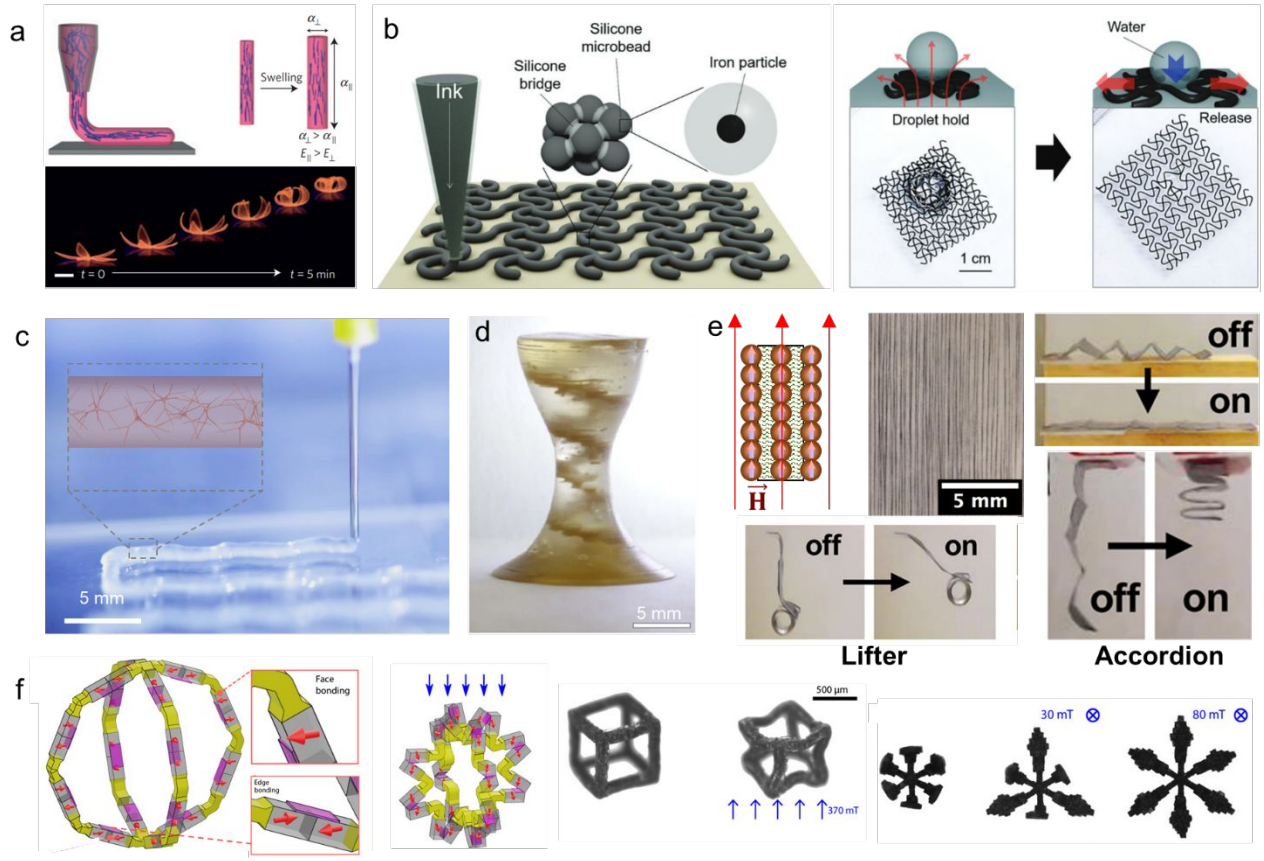

Figure 7: a) Example of biomimetic 4D printing and the folding of the structures upon swelling. Reproduced with permission from ref. [186]. Copyright 2016, Nature Publishing Group. **b)** 3D printing of homocomposite magnetic ink made of silicone and mesh actuation on water surface by magnetic field. Reproduced with permission from ref. [188]. Copyright 2019, Wiley-VCH. **c)** 3D printing of sodium alginate homocomposite ink. The molecular alginate hydrogel is reinforced with soft dendritic colloids also made of alginate. Reproduced with permission from ref. [201]. **d)** Magnetic field-assisted 3D printing. Reproduced with permission from ref. [202]. **e)** Composite soft actuators made by embedding in elastomeric matrix pre-assembled chains of iron microparticles. Reproduced with permission from ref. [203]. Copyright 2017, American Physical Society. **f)** 3D miniature magnetic soft structures by heterogenous assembly using voxels of different magnetic moments. Reproduced with permission from ref. [204]. Copyright 2021, AAAS.

Due to the rapid shape reconfiguration and untethered manipulation, magnetic field-directed 3D printed structures are a suitable core of soft actuators and soft robotics. The mechanical response of these structures can be programmed by the 3D printed structure and modulated by the remotely applied fields. Our group used the homocomposite capillary inks mentioned earlier as a

Soft Matter

basis of 3D printed soft magneto-capillary actuators.[118,188] We embedded carbonyl iron particles into the silicone microbeads by adding the particles to the silicone droplets before curing (**Figure 7b left**). The cured composite microbeads were bound by liquid silicone into capillary paste. The final 3D-printed and crosslinked silicone meshes are hydrophobic and thus can be suspended on the surface of water while supported by interfacial tension. These floating meshes can be actuated by the joint action of magnetic field and lateral capillary interactions. 3D printed structures were floated at the interface between air and water held in Petri dish. When magnetic field (with an attractive gradient) was applied from below the dish, the floating mesh was pulled down, while the increasing lateral capillary attraction led to mesh re-configuration and compression. The compression patterns were determined by spatial design of the meshes. The reconfiguration outcomes depended on the mesh patterns, including auxetic type lattices and droplet microdispensers (**Figure 7b right**). Another example of 3D printed homocomposite hydrogel made in our lab, where both the primary matrix and the reinforcement networks are made of sodium alginate, is shown in **Figure 7c**.[201] The hydrogels are reinforced by a second colloidal networks made of fibrillar branched alginate soft dendritic colloids. The printed colloidal-molecular network hydrogel shows better mechanical characteristics (storage modulus, Young's modulus) than either constitutive networks at the same concentration.

Kokkinis et al. reported how the 3D printing of composite materials can be enhanced by magnetic field (**Figure 7d**).[202] They incorporated alumina platelets as texturable particles into polyurethane acrylate based ink. After ink ejection, the orientation of the platelets was guided by the application of an external magnetic field, giving rise to internal microstructural features. Kim et al. demonstrated in situ magnetic field-assisted 3D printing of magnetic actuators.[190] Ferromagnetic microparticles embedded in a silicone ink were polarized during extrusion; thus, the magnetic polarization pattern was embedded in the filament domains, which in turn enables programmable shape reconfiguration. Further, it has been shown that applying a magnetic field during extrusion-based 3D printing can control the rheology of the ink containing magnetic nanoparticles by increasing the microstructural strength of the final structures.[205] This is a result of the field-induced interactions between the solid particles leading to chain or cluster formation. The viscosity of MR fluids generally increases with applied magnetic field, therefore incorporating MR fluids in the elastomer matrix during 3D printing can also alter the mechanical properties of the printed structures.

Magnetically responsive smart composite materials can also be synthesized by assembling magnetic nanoparticles and microparticles from suspension under applied fields into various configurations as discussed in Sections 2 and 3, and then incorporating these assemblies into a soft

Soft Matter

polymer matrix by solvent casting and bulk polymerization. The organized magnetic particles embedded into soft matrix yield magnetoactive elastomers (MAE).[203,204,206] The soft matrix can be made of thermoplastic polyurethane,[207] PDMS,[118] PNIPAM[208,209] or even agarose hydrogel. Such MAE composites are subject to strong torque and bending in magnetic fields as the embedded chains try to align with the direction of the applied field. Thus, one can fabricate permanent materials which can be macroscopically guided depending on the particle structure assembled within the composites.[210–213] For example, Shmauch et al. used solvent casting method to embed magnetic field-aligned microparticles in an elastomer film. The resulting composite film was strongly and directionally responsive to an externally applied magnetic field.[203,207] This programmed response to an external magnetic field was used to demonstrate soft robotic actuation in applications such as valves, "arms" that can lift up to 50× the matrix weight, and accordion folds that can stretch and contact (**Figure 7e**).

Recent advances in the design and assembly of complex magnetically actuatable structures also involve the making and assembly of soft microscale units also known as "voxels," as building blocks of the soft machines. For example, Zhang et al. introduced a bottom-up assembly approach to fabricate small-scale 3D soft-bodied machines with high spatial resolution, which respond to magnetic fields. Their fabrication is based on a 3D heterogeneous integration approach with printed elastomeric voxels (**Figure7f**).[204,214] These authors demonstrate complex shapes with directional magnetic response and reconfiguration. Such comprehensive structures made of pre-designed units have promise for numerous applications in future biomedical practice.

Summary and outlook

This perspective illustrates the extremely rich variety of flexible and responsive colloidal structures that encompass variations of magnetic and capillary interactions. Both of these interactions represent valuable tools in the "interaction toolbox" that can be used to assemble and manipulate reconfigurable soft matter. This is a result of a few characteristics that are common for both magnetic and capillary interactions: (1) They are extremely long ranged and "soft" on the colloidal scale. Unlike the omnipresent electrostatic and van der Waals interactions which operate on distances up to tens of nanometers, the magnetic and capillary interactions could extend to distances of hundreds of microns or even millimeters. Their decay with distance, d, is commonly expressed as proportional to d^{-2}. (2) The capillary attraction is also unique in that it does not lead to irreversible adhesion of the particles and allows their re-configuration even when strongly held together by the capillary menisci. (3) They could either be unidirectional or strongly oriented. The dipolar and gradient driven magnetic attraction are strongly dependent on the particle orientation

Soft Matter

and position, while many capillary interactions can be strongly specific. However, both interactions can operate on particles in near unform fields or sloped menisci. (4) They could be reversible or reconfigurable. The interactions can be easily turned on and off on demand, but turning on the magnetic field, or adding more liquid, or surfactants for the case of capillary forces. (5) Last, but not least, they are simple to implement. The magnetic fields can be applied efficiently and reliably across many colloidal and biomedical targets using sets of electronically switched electromagnets. The field magnitude and gradient directions are easily controlled and modelled.

These convenient, controllable, and predictable interactions have found many applications, exemplified in this paper. The rich variety of structures reviewed here by no means exhaust all the possible applications or physical effects enabled by capillarity and magnetic field actuation in the formation and manipulation of soft matter systems. For example, one can add the element of active motility in such systems, making the particles travel along pre-designed trajectories before assembly by using the Marangoni effect of interfacial propulsion driven by release of surface-active species.[215,216] Given the continuing interest and expanding scope of investigation of reconfigurable, actuatable, and "active" soft matter, one can expect that the use of the capillary and magnetic interactions as simple and efficient means of making flexible and responsive assemblies will continue to enable exciting new scientific advances.

Acknowledgements

This paper is gratefully dedicated to the memory of Prof. Peter Kralchevsky, an outstanding scientist, who made seminal contributions to the theories of capillary forces and colloidal interactions. The authors acknowledge support from NSF grants CBET-1935248, CBET-2133983 and partially CMMI-1825476.

Conflicts of interest

There are no conflicts of interest to declare.

Keywords

Magnetic, capillary, assembly, responsive, 3D printing

References

1 J. N. Israelachvili, D. J. Mitchell and B. W. Ninham, *BBA - Biomembr.*, 1977, **470**, 185–201

Soft Matter

doi:10.1016/0005-2736(77)90099-2.

2 X. Cui, S. Mao, M. Liu, H. Yuan and Y. Du, *Langmuir*, 2008, **24**, 10771–10775 doi:10.1021/la801705y.

3 B. Gold, *Mol. Diagnostics Second Ed.*, 2009, 501–511 doi:10.1016/B978-0-12-374537-8.00034-1.

4 J. Hernández-Rojas, D. Chakrabarti and D. J. Wales, *Phys. Chem. Chem. Phys.*, 2016, **18**, 26579–26585 doi:10.1039/c6cp03085h.

5 S. C. Glotzer, M. J. Solomon and N. A. Kotov, *AIChE J.*, 2004, **50**, 2978–2985 doi:10.1002/aic.10413.

6 A. M. Kalsin, M. Fialkowski, M. Paszewski, S. K. Smoukov, K. J. M. Bishop and B. A. Grzybowski, *Science (80-.).*, 2006, **312**, 420–424 doi:10.1126/science.1125124.

7 B. G. Prevo, D. M. Kuncicky and O. D. Velev, *Colloids Surfaces A Physicochem. Eng. Asp.*, 2007, **311**, 2–10 doi:10.1016/j.colsurfa.2007.08.030.

8 O. D. Velev, N. D. Denkov, P. A. Kralchevsky, I. B. Ivanov, H. Yoshimura and K. Nagayama, *Prog. Colloid Polym. Sci.*, 1993, **93**, 366–367 doi:10.1007/bfb0118623.

9 B. Bharti and O. D. Velev, *Langmuir*, 2015, **31**, 7897–7908 doi:10.1021/la504793y.

10 S. K. Smoukov, S. Gangwal, M. Marquez and O. D. Velev, *Soft Matter*, 2009, **5**, 1285–1292 doi:10.1039/b814304h.

11 K. Han, C. W. Shields, N. M. Diwakar, B. Bharti, G. P. López and O. D. Velev, *Sci. Adv.*, 2017, **3**, 1–7 doi:10.1126/sciadv.1701108.

12 K. Han, C. W. Shields and O. D. Velev, *Adv. Funct. Mater.*, 2018, **28**, 1705953 doi:10.1002/adfm.201705953.

13 A. Al Harraq, J. G. Lee and B. Bharti, *Sci. Adv.*, 2020, **6**, 5337–5345 doi:10.1126/sciadv.aba5337.

14 S. Gangwal, O. J. Cayre and O. D. Velev, *Langmuir*, 2008, **24**, 13312–13320 doi:10.1021/la8015222.

15 J. P. Singh, P. P. Lele, F. Nettesheim, N. J. Wagner and E. M. Furst, *Phys. Rev. E*, 2009, **79**, 050401 doi:10.1103/PhysRevE.79.050401.

16 D. Nagao, M. Sugimoto, A. Okada, H. Ishii, M. Konno, A. Imhof and A. Van Blaaderen, *Langmuir*, 2012, **28**, 6546–6550 doi:10.1021/la204493m.

17 R. S. Hendley, L. Zhang and M. A. Bevan, *Soft Matter*, 2022, **18**, 9273–9282 doi:10.1039/D2SM01078J.

18 X. Chen, L. Lin, Z. Li and H. B. Sun, *Adv. Funct. Mater.*, 2022, **32**, 2104649 doi:10.1002/adfm.202104649.

19 J. Zhang, J. Guo, F. Mou and J. Guan, *Micromachines*, 2018, **9**, 88 doi:10.3390/mi9020088.

20 S. J. Boehm, L. Lin, K. Guzmán Betancourt, R. Emery, J. S. Mayer, T. S. Mayer and C. D. Keating, *Langmuir*, 2015, **31**, 5779–5786 doi:10.1021/acs.langmuir.5b01633.

21 O. D. Velev and K. H. Bhatt, *Soft Matter*, 2006, **2**, 738–750 doi:10.1039/b605052b.

Soft Matter

22 M. Grzelczak, J. Vermant, E. M. Furst and L. M. Liz-Marzán, *ACS Nano*, 2010, **4**, 3591–3605 doi:10.1021/nn100869j.

23 V. Liljeström, C. Chen, P. Dommersnes, J. O. Fossum and A. H. Gröschel, *Curr. Opin. Colloid Interface Sci.*, 2019, **40**, 25–41 doi:10.1016/j.cocis.2018.10.008.

24 Z. Li, F. Yang and Y. Yin, *Adv. Funct. Mater.*, 2020, **30**, 1903467 doi:10.1002/adfm.201903467.

25 Z. Nie, D. Fava, E. Kumacheva, S. Zou, G. C. Walker and M. Rubinstein, *Nat. Mater.*, 2007, **6**, 609–614 doi:10.1038/nmat1954.

26 Q. Chen, J. Yan, J. Zhang, S. C. Bae and S. Granick, *Langmuir*, 2012, **28**, 13555–13561 doi:10.1021/la302226w.

27 S. C. Glotzer and M. J. Solomon, *Nat. Mater.*, 2007, **6**, 557–562 doi:10.1038/nmat1949.

28 S. R. Mishra, M. D. Dickey, O. D. Velev and J. B. Tracy, *Nanoscale*, 2016, **8**, 1309–1313 doi:10.1039/c5nr07410j.

29 M. Wang, L. He and Y. Yin, *Mater. Today*, 2013, **16**, 110–116 doi:10.1016/j.mattod.2013.04.008.

30 R. M. Erb, H. S. Son, B. Samanta, V. M. Rotello and B. B. Yellen, *Nature*, 2009, **457**, 999–1002 doi:10.1038/nature07766.

31 J. Yan, S. C. Bae and S. Granick, *Adv. Mater.*, 2015, **27**, 874–879 doi:10.1002/adma.201403857.

32 N. Osterman, I. Poberaj, J. Dobnikar, D. Frenkel, P. Ziherl and D. Babić, *Phys. Rev. Lett.*, DOI:10.1103/PhysRevLett.103.228301 doi:10.1103/PhysRevLett.103.228301.

33 I. B. Liu, N. Sharifi-Mood and K. J. Stebe, *Annu. Rev. Condens. Matter Phys.*, 2018, **9**, 283–305 doi:10.1146/annurev-conmatphys-031016-025514.

34 L. Botto, E. P. Lewandowski, M. Cavallaro and K. J. Stebe, *Soft Matter*, 2012, **8**, 9957–9971 doi:10.1039/c2sm25929j.

35 S. Ni, L. Isa and H. Wolf, *Soft Matter*, 2018, **14**, 2978–2995 doi:10.1039/c7sm02496g.

36 A. Snezhko and I. S. Aranson, *Nat. Mater.*, 2011, **10**, 698–703 doi:10.1038/nmat3083.

37 A. Snezhko, I. S. Aranson and W. K. Kwok, *Phys. Rev. Lett.*, DOI:10.1103/PhysRevLett.96.078701 doi:10.1103/PhysRevLett.96.078701.

38 G. B. Davies, T. Krüger, P. V. Coveney, J. Harting and F. Bresme, *Adv. Mater.*, 2014, **26**, 6715–6719 doi:10.1002/adma.201402419.

39 B. Bharti, A. L. Fameau, M. Rubinstein and O. D. Velev, *Nat. Mater.*, 2015, **14**, 1104–1109 doi:10.1038/nmat4364.

40 P. Moritz, A. Gonon, T. Blon, N. Ratel-Ramond, F. Mathieu, P. Farger, J. M. Asensio-Revert, S. Cayez, D. Bourrier, D. Saya, L. Nicu, G. Viau, T. Leïchlé and L. M. Lacroix, *ACS Nano*, 2021, **15**, 5096–5108 doi:10.1021/acsnano.0c10215.

41 J. Faraudo, J. S. Andreu and J. Camacho, *Soft Matter*, 2013, **9**, 6654–6664 doi:10.1039/c3sm00132f.

42 J. H. E. Promislow, A. P. Gast and M. Fermigier, *J. Chem. Phys.*, 1995, **102**, 5492–5498

Soft Matter

doi:10.1063/1.469278.

43 C. P. Reynolds, K. E. Klop, F. A. Lavergne, S. M. Morrow, D. G. A. L. Aarts and R. P. A. Dullens, *J. Chem. Phys.*, 2015, **143**, 214903 doi:10.1063/1.4936323.

44 J. Ge, H. Lee, L. He, J. Kim, Z. Lu, H. Kim, J. Goebl, S. Kwon and Y. Yin, *J. Am. Chem. Soc.*, 2009, **131**, 15687–15694 doi:10.1021/ja903626h.

45 Y. Hu, L. He and Y. Yin, *Angew. Chemie - Int. Ed.*, 2011, **50**, 3747–3750 doi:10.1002/anie.201100290.

46 L. He, M. Wang, J. Ge and Y. Yin, *Acc. Chem. Res.*, 2012, **45**, 1431–1440 doi:10.1021/ar200276t.

47 S. L. Biswal and A. P. Gast, *Phys. Rev. E - Stat. Physics, Plasmas, Fluids, Relat. Interdiscip. Top.*, 2004, **69**, 9 doi:10.1103/PhysRevE.69.041406.

48 E. M. Furst, C. Suzuki, M. Fermigier and A. P. Gast, *Langmuir*, 1998, **14**, 7334–7336 doi:10.1021/la980703i.

49 J. Byrom, P. Han, M. Savory and S. L. Biswal, *Langmuir*, 2014, **30**, 9045–9052 doi:10.1021/la5009939.

50 M. Fermigier and A. P. Gast, *J. Colloid Interface Sci.*, 1992, **154**, 522–539 doi:10.1016/0021-9797(92)90165-I.

51 E. M. Furst and A. P. Gast, *Phys. Rev. E - Stat. Physics, Plasmas, Fluids, Relat. Interdiscip. Top.*, 2000, **62**, 6916–6925 doi:10.1103/PhysRevE.62.6916.

52 J. M. Laskar, J. Philip and B. Raj, *Phys. Rev. E - Stat. Nonlinear, Soft Matter Phys.*, 2009, **80**, 041401 doi:10.1103/PhysRevE.80.041401.

53 Y. Nagaoka, H. Morimoto and T. Maekawa, *Langmuir*, 2011, **27**, 9160–9164 doi:10.1021/la201156q.

54 J. H. E. Promislow and A. P. Gast, *Langmuir*, 1996, **12**, 4095–4102 doi:10.1021/la960104g.

55 J. W. Swan, J. L. Bauer, Y. Liu and E. M. Furst, *Soft Matter*, 2014, **10**, 1102–1109 doi:10.1039/c3sm52663a.

56 N. Osterman, D. Babič, I. Poberaj, J. Dobnikar and P. Ziherl, *Phys. Rev. Lett.*, 2007, **99**, 248301 doi:10.1103/PhysRevLett.99.248301.

57 P. J. Camp, *Phys. Rev. E - Stat. Physics, Plasmas, Fluids, Relat. Interdiscip. Top.*, 2003, **68**, 061506 doi:10.1103/PhysRevE.68.061506.

58 G. Malescio and G. Pellicane, *Nat. Mater.*, 2003, **2**, 97–100 doi:10.1038/nmat820.

59 A. K. Vuppu, A. A. Garcia and M. A. Hayes, *Langmuir*, 2003, **19**, 8646–8653 doi:10.1021/la034195a.

60 S. Melle, G. G. Fuller and M. A. Rubio, *Phys. Rev. E*, 2000, **61**, 4111–4117 doi:10.1103/PhysRevE.61.4111.

61 D. H. De Jong, G. Singh, W. F. D. Bennett, C. Arnarez, T. A. Wassenaar, L. V. Schäfer, X. Periole, D. P. Tieleman and S. J. Marrink, *J. Chem. Theory Comput.*, 2013, **9**, 687–697

Soft Matter

doi:10.1021/ct300646g.

62 J. E. Martin, R. A. Anderson and C. P. Tigges, *J. Chem. Phys.*, 1999, **110**, 4854–4866 doi:10.1063/1.478389.

63 J. E. Martin, R. A. Anderson and C. P. Tigges, *J. Chem. Phys.*, 1998, **108**, 7887–7900 doi:10.1063/1.476226.

64 T. G. Kang, M. A. Hulsen, P. D. Anderson, J. M. J. Den Toonder and H. E. H. Meijer, *Phys. Rev. E*, 2007, **76**, 066303 doi:10.1103/PhysRevE.76.066303.

65 I. Petousis, E. Homburg, R. Derks and A. Dietzel, *Lab Chip*, 2007, **7**, 1746–1751 doi:10.1039/b713735b.

66 T. Yang, B. Sprinkle, Y. Guo, J. Qian, D. Hua, A. Donev, D. W. M. Marr and N. Wu, *Proc. Natl. Acad. Sci. U. S. A.*, 2020, **117**, 18186–18193 doi:10.1073/pnas.2007255117.

67 P. Vázquez-Montejo, J. M. Dempster and M. O. De La Cruz, *Phys. Rev. Mater.*, 2017, **1**, 064402 doi:10.1103/PhysRevMaterials.1.064402.

68 K. Zahn, R. Lenke and G. Maret, *Phys. Rev. Lett.*, 1999, **82**, 2721–2724 doi:10.1103/PhysRevLett.82.2721.

69 E. Hilou, D. Du, S. Kuei and S. L. Biswal, *Phys. Rev. Mater.*, 2018, **2**, 025602 doi:10.1103/PhysRevMaterials.2.025602.

70 E. Hilou, K. Joshi and S. L. Biswal, *Soft Matter*, 2020, **16**, 8799–8805 doi:10.1039/d0sm01100b.

71 E. Yammine, E. Souaid, S. Youssef, M. Abboud, S. Mornet, M. Nakhl and E. Duguet, *Part. Part. Syst. Charact.*, 2020, **37**, 1–12 doi:10.1002/ppsc.202000111.

72 S. Ravaine and E. Duguet, *Curr. Opin. Colloid Interface Sci.*, 2017, **30**, 45–53 doi:10.1016/j.cocis.2017.05.002.

73 W. Li, H. Palis, R. Mérindol, J. Majimel, S. Ravaine and E. Duguet, *Chem. Soc. Rev.*, 2020, **49**, 1955–1976 doi:10.1039/c9cs00804g.

74 A. B. Pawar and I. Kretzschmar, *Macromol. Rapid Commun.*, 2010, **31**, 150–168 doi:10.1002/marc.200900614.

75 A. K. Pearce, T. R. Wilks, M. C. Arno and R. K. O'Reilly, *Nat. Rev. Chem.*, 2021, **5**, 21–45 doi:10.1038/s41570-020-00232-7.

76 D. Lisjak and A. Mertelj, *Prog. Mater. Sci.*, 2018, **95**, 286–328 doi:10.1016/j.pmatsci.2018.03.003.

77 J. A. Champion, Y. K. Katare and S. Mitragotri, *Proc. Natl. Acad. Sci. U. S. A.*, 2007, **104**, 11901–11904 doi:10.1073/pnas.0705326104.

78 Z. Wang, Z. Wang, J. Li, S. T. H. Cheung, C. Tian, S. H. Kim, G. R. Yi, E. Ducrot and Y. Wang, *J. Am. Chem. Soc.*, 2019, **141**, 14853–14863 doi:10.1021/jacs.9b07785.

79 C. Wyatt Shields Iv, S. Zhu, Y. Yang, B. Bharti, J. Liu, B. B. Yellen, O. D. Velev and G. P. López, *Soft Matter*, 2013, **9**, 9219–9229 doi:10.1039/c3sm51119g.

Soft Matter

80 M. N. Popescu, *Langmuir*, 2020, **36**, 6861–6870 doi:10.1021/acs.langmuir.9b03973.

81 J. Hu, S. Zhou, Y. Sun, X. Fang and L. Wu, *Chem. Soc. Rev.*, 2012, **41**, 4356–4378 doi:10.1039/c2cs35032g.

82 E. Poggi and J. F. Gohy, *Colloid Polym. Sci.*, 2017, **295**, 2083–2108 doi:10.1007/s00396-017-4192-8.

83 A. Walther and A. H. E. Müller, *Chem. Rev.*, 2013, **113**, 5194–5261 doi:10.1021/cr300089t.

84 G. Loget and A. Kuhn, *J. Mater. Chem.*, 2012, **22**, 15457–15474 doi:10.1039/c2jm31740k.

85 E. Yammine, E. Souaid, S. Youssef, M. Abboud, S. Mornet, M. Nakhl and E. Duguet, *Part. Part. Syst. Charact.*, 2020, **37**, 2000111 doi:10.1002/ppsc.202000111.

86 B. Ren, A. Ruditskiy, J. H. Song and I. Kretzschmar, *Langmuir*, 2012, **28**, 1149–1156 doi:10.1021/la203969f.

87 J. Yan, S. C. Bae and S. Granick, *Adv. Mater.*, 2015, **27**, 874–879 doi:10.1002/adma.201403857.

88 J. Yan, M. Bloom, S. C. Bae, E. Luijten and S. Granick, *Nature*, 2012, **491**, 578–581 doi:10.1038/nature11619.

89 K. P. Herlihy, J. Nunes and J. M. DeSimone, *Langmuir*, 2008, **24**, 8421–8426 doi:10.1021/la801250g.

90 J. P. Rolland, B. W. Maynor, L. E. Euliss, A. E. Exner, G. M. Denison and J. M. DeSimone, *J. Am. Chem. Soc.*, 2005, **127**, 10096–10100 doi:10.1021/ja051977c.

91 C. W. Shields, Y.-K. Kim, K. Han, A. C. Murphy, A. J. Scott, N. L. Abbott and O. D. Velev, *Adv. Intell. Syst.*, 2020, **2**, 1900114 doi:10.1002/aisy.201900114.

92 K. Han, C. W. Shields, B. Bharti, P. E. Arratia and O. D. Velev, *Langmuir*, 2020, **36**, 7148–7154 doi:10.1021/acs.langmuir.9b03698.

93 J. Yan, K. Chaudhary, S. Chul Bae, J. A. Lewis and S. Granick, *Nat. Commun.*, 2013, **4**, 1–9 doi:10.1038/ncomms2520.

94 E. Guzmán, F. Ortega and R. G. Rubio, *Langmuir*, 2022, **38**, 13313–13321 doi:10.1021/acs.langmuir.2c02038.

95 H. J. Butt, *Langmuir*, 2008, **24**, 4715–4721 doi:10.1021/la703640f.

96 L. Yao, L. Botto, M. Cavallaro, B. J. Bleier, V. Garbin and K. J. Stebe, *Soft Matter*, 2012, **9**, 779–786 doi:10.1039/C2SM27020J.

97 B. J. Park and E. M. Furst, *Soft Matter*, 2011, **7**, 7676–7682 doi:10.1039/C1SM00005E.

98 A. Kumar, B. J. Park, F. Tu and D. Lee, *Soft Matter*, 2013, **9**, 6604–6617 doi:10.1039/C3SM50239B.

99 P. A. Kralchevsky, N. D. Denkov and K. D. Danov, *Langmuir*, 2001, **17**, 7694–7705 doi.org/10.1021/la0109359.

100 P. A. Kralchevsky, V. N. Paunov, N. D. Denkov, I. B. Ivanov and K. Nagayama, *J. Colloid Interface Sci.*, 1993, **155**, 420–437 doi:10.1006/jcis.1993.1056.

Soft Matter

101 P. A. Kralchevsky, V. N. Paunov, I. B. Ivanov and K. Nagayama, *J. Colloid Interface Sci.*, 1992, **151**, 79–94 doi:10.1016/0021-9797(92)90239-I.

102 P. A. Kralchevsky and K. Nagayama, *Adv. Colloid Interface Sci.*, 2000, **85**, 145–192 doi:10.1016/S0001-8686(99)00016-0.

103 P. A. Kralchevsky and K. Nagayama, *Langmuir*, 1994, **10**, 23–36 doi:10.1021/la00013a004.

104 P. A. Kralchevsky and N. D. Denkov, *Curr. Opin. Colloid Interface Sci.*, 2001, **6**, 383–401 doi:10.1016/S1359-0294(01)00105-4.

105 F. Bresme and M. Oettel, *J. Phys. Condens. Matter*, 2007, **19**, 413101 doi:10.1088/0953-8984/19/41/413101.

106 Y. Lin, H. Skaff, T. Emrick, A. D. Dinsmore and T. P. Russell, *Science (80-.).*, 2003, **299**, 226–229 doi:10.1126/science.1078616.

107 B. G. Prevo and O. D. Velev, *Langmuir*, 2004, **20**, 2099–2107 doi:10.1021/la035295j.

108 B. G. Prevo, Y. Hwang and O. D. Velev, *Chem. Mater.*, 2005, **17**, 3642–3651 doi:10.1021/cm050416h.

109 V. N. Paunov, P. A. Kralchevsky, N. D. Denkov and K. Nagayama, *J. Colloid Interface Sci.*, 1993, **157**, 100–112 doi:10.1006/jcis.1993.1163.

110 V. N. Paunov, P. A. Kralchevsky, N. D. Denkov, I. B. Ivanov and K. Nagayama, *Colloids and Surfaces*, 1992, **67**, 119–138 doi:10.1016/0166-6622(92)80292-A.

111 P. A. Kralchevsky and V. N. Paunov, *J. Fluid Mech.*, 1995, **299**, 105–132 doi:10.1017/S0022112095003442.

112 D. Y. C. Chan, J. D. Henry and L. R. White, *J. Colloid Interface Sci.*, 1981, **79**, 410–418 doi:10.1016/0021-9797(81)90092-8.

113 J. C. Loudet, A. M. Alsayed, J. Zhang and A. G. Yodh, *Phys. Rev. Lett.*, 2005, **94**, 018301 doi:10.1103/PhysRevLett.94.018301.

114 E. P. Lewandowski, M. Cavallaro, L. Botto, J. C. Bernate, V. Garbin and K. J. Stebe, *Langmuir*, 2010, **26**, 15142–15154 doi:10.1021/la1012632.

115 S. Zhao, Y. Wu, W. Lu and B. Liu, *ACS Macro Lett.*, 2019, **8**, 363–367 doi:10.1021/acsmacrolett.8b00985.

116 B. Bharti, D. Rutkowski, K. Han, A. U. Kumar, C. K. Hall and O. D. Velev, *J. Am. Chem. Soc.*, 2016, **138**, 14948–14953 doi:10.1021/jacs.6b08017.

117 E. Koos, *Curr. Opin. Colloid Interface Sci.*, 2014, **19**, 575–584 doi:10.1016/j.cocis.2014.10.004.

118 S. Roh, D. P. Parekh, B. Bharti, S. D. Stoyanov and O. D. Velev, *Adv. Mater.*, 2017, **29**, 1701554 doi:10.1002/adma.201701554.

119 E. Koos, J. Johannsmeier, L. Schwebler and N. Willenbacher, *Soft Matter*, 2012, **8**, 6620–6628 doi:10.1039/c2sm25681a.

120 N. Bowden, A. Terfort, J. Carbeck and G. M. Whitesides, *Science (80-.).*, 1997, **276**, 233–235

Soft Matter

doi:10.1126/science.276.5310.233.

121 N. Bowden, F. Arias, T. Deng and G. M. Whitesides, *Langmuir*, 2001, **17**, 1757–1765 doi:10.1021/la001447o.

122 L. Botto, L. Yao, R. L. Leheny and K. J. Stebe, *Soft Matter*, 2012, **8**, 4971–4979 doi:10.1039/c2sm25211b.

123 B. Madivala, J. Fransaer and J. Vermant, *Langmuir*, 2009, **25**, 2718–2728 doi:10.1021/la803554u.

124 Q. Wang, J. Yu, K. Yuan, L. Yang, D. Jin and L. Zhang, *Appl. Mater. Today*, 2020, **18**, 100489 doi:10.1016/j.apmt.2019.100489.

125 F. Li, S. A. Delo and A. Stein, *Angew. Chemie*, 2007, **119**, 6786–6789 doi:10.1002/ange.200701553.

126 X. Zheng, M. Liu, M. He, D. J. Pine and M. Weck, *Angew. Chemie - Int. Ed.*, 2017, **56**, 5507–5511 doi:10.1002/anie.201701456.

127 L. Tian, Y. Liu, D. Wang, J. Tan, Y. Xie, B. Li, Q. Zhang, C. Zhu and J. Xu, *Polym. Chem.*, 2022, **13**, 1084–1089 doi:10.1039/d1py00360g.

128 D. J. Kraft, W. S. Vlug, C. M. Van Kats, A. Van Blaaderen, A. Imhof and W. K. Kegel, *J. Am. Chem. Soc.*, 2009, **131**, 1182–1186 doi:10.1021/ja8079803.

129 E. Koos and N. Willenbacher, *Science (80-.).*, 2011, **331**, 897–900 doi:10.1126/science.1199243.

130 H. Ding, S. Barg and B. Derby, *Nanoscale*, 2020, **12**, 11440–11447 doi:10.1039/c9nr10831a.

131 S. Van Kao, L. E. Nielsen and C. T. Hill, *J. Colloid Interface Sci.*, 1975, **53**, 367–373 doi:10.1016/0021-9797(75)90052-1.

132 F. Bossler and E. Koos, *Langmuir*, 2016, **32**, 1489–1501 doi:10.1021/acs.langmuir.5b04246.

133 F. Bossler, L. Weyrauch, R. Schmidt and E. Koos, *Colloids Surfaces A Physicochem. Eng. Asp.*, 2017, **518**, 85–97 doi:10.1016/j.colsurfa.2017.01.026.

134 S. Hoffmann, E. Koos and N. Willenbacher, *Food Hydrocoll.*, 2014, **40**, 44–52 doi:10.1016/j.foodhyd.2014.01.027.

135 J. Allard, S. Burgers, M. C. Rodríguez González, Y. Zhu, S. De Feyter and E. Koos, *Colloids Surfaces A Physicochem. Eng. Asp.*, 2022, **648**, 129224 doi:10.1016/j.colsurfa.2022.129224.

136 M. Schneider, E. Koos and N. Willenbacher, *Sci. Rep.*, 2016, **6**, 1–10 doi:10.1038/srep31367.

137 J. Maurath and N. Willenbacher, *J. Eur. Ceram. Soc.*, 2017, **37**, 4833–4842 doi:10.1016/j.jeurceramsoc.2017.06.001.

138 M. L. Sesso, S. Slater, J. Thornton and G. V. Franks, *J. Am. Ceram. Soc.*, 2021, **104**, 4977–4990 doi:10.1111/jace.17911.

139 B. A. Grzybowski, H. A. Stone and G. M. Whitesides, *Nature*, 2000, **405**, 1033–1036 doi:10.1038/35016528.

140 G. Grosjean, M. Hubert, Y. Collard, A. Sukhov, J. Harting, A. S. Smith and N. Vandewalle, *Soft Matter*, 2019, **15**, 9093–9103 doi:10.1039/c9sm01414d.

Soft Matter

141 M. Belkin, A. Snezhko, I. S. Aranson and W. K. Kwok, *Phys. Rev. Lett.*, 2007, **99**, 158301 doi:10.1103/PhysRevLett.99.158301.

142 A. Snezhko, I. S. Aranson and W. K. Kwok, *Phys. Rev. E - Stat. Nonlinear, Soft Matter Phys.*, 2006, **73**, 041306 doi:10.1103/PhysRevE.73.041306.

143 J. Dobnikar, A. Snezhko and A. Yethiraj, *Soft Matter*, 2013, **9**, 3693–3704 doi:10.1039/c3sm27363f.

144 A. Snezhko and I. S. Aranson, *Nat. Mater.*, 2011, **10**, 698–703 doi:10.1038/nmat3083.

145 Q. Xie and J. Harting, *Adv. Mater.*, 2021, **33**, 2006390 doi:10.1002/adma.202006390.

146 G. B. Davies, T. Krüger, P. V. Coveney, J. Harting and F. Bresme, *Soft Matter*, 2014, **10**, 6742–6748 doi:10.1039/c4sm01124d.

147 J. Faraudo and F. Bresme, *J. Chem. Phys.*, 2003, **118**, 6518–6528 doi:10.1063/1.1559728.

148 F. Bresme and J. Faraudo, *J. Phys. Condens. Matter*, 2007, **19**, 375110 doi:10.1088/0953-8984/19/37/375110.

149 Q. Xie, G. B. Davies, F. Günther and J. Harting, *Soft Matter*, 2015, **11**, 3581–3588 doi:10.1039/c5sm00255a.

150 Q. Xie, G. B. Davies and J. Harting, *Soft Matter*, 2016, **12**, 6566–6574 doi:10.1039/c6sm01201a.

151 B. Bharti, A. L. Fameau and O. D. Velev, *Faraday Discuss.*, 2015, **181**, 437–448 doi:10.1039/c4fd00272e.

152 J. Zhou, L. Wang, X. Qiao, B. P. Binks and K. Sun, *J. Colloid Interface Sci.*, 2012, **367**, 213–224 doi:10.1016/j.jcis.2011.11.001.

153 J. Zhou, X. Qiao, B. P. Binks, K. Sun, M. Bai, Y. Li and Y. Liu, *Langmuir*, 2011, **27**, 3308–3316 doi:10.1021/la1036844.

154 A. L. Fameau, A. Carl, A. Saint-Jalmes and R. Von Klitzing, *ChemPhysChem*, 2015, **16**, 66–75 doi:10.1002/cphc.201402580.

155 D. Davino, M. D'auria, R. Pantani and L. Sorrentino, *Polymers (Basel).*, 2021, **23**, 1–18 doi:10.3390/polym13010024.

156 J. A. Rodrigues, E. Rio, J. Bobroff, D. Langevin and W. Drenckhan, *Colloids Surfaces A Physicochem. Eng. Asp.*, 2011, **384**, 408–416 doi:10.1016/j.colsurfa.2011.04.029.

157 K. Soetanto and H. Watarai, *Japanese J. Appl. Physics, Part 1 Regul. Pap. Short Notes Rev. Pap.*, 2000, **39**, 3230–3232 doi:10.1143/jjap.39.3230.

158 A. L. Campbell, S. D. Stoyanov and V. N. Paunov, *Soft Matter*, 2009, **5**, 1019–1023 doi:10.1039/b812706a.

159 X. Zhao, P. A. Quinto-Su and C. D. Ohl, *Phys. Rev. Lett.*, 2009, **102**, 024501 doi:10.1103/PhysRevLett.102.024501.

160 A. L. Fameau and S. Fujii, *Curr. Opin. Colloid Interface Sci.*, 2020, **50**, 101380 doi:10.1016/j.cocis.2020.08.005.

Soft Matter

161 S. Hutzler, D. Weaire, F. Eliás and E. Janiaud, *Philos. Mag. Lett.*, 2002, **82**, 297–301 doi:10.1080/09500830210128074.

162 E. Blanco, S. Lam, S. K. Smoukov, K. P. Velikov, S. A. Khan and O. D. Velev, *Langmuir*, 2013, **29**, 10019–10027 doi:10.1021/la4014224.

163 A. L. Fameau, S. Lam and O. D. Velev, *Chem. Sci.*, 2013, **4**, 3874–3881 doi:10.1039/c3sc51774h.

164 N. I. Castellanos, B. Bharti and O. D. Velev, *J. Phys. Chem. B*, 2021, **125**, 7900–7910 doi:10.1021/acs.jpcb.1c03158.

165 S. Lam, E. Blanco, S. K. Smoukov, K. P. Velikov and O. D. Velev, *J. Am. Chem. Soc.*, 2011, **133**, 13856–13859 doi:10.1021/ja205065w.

166 A. Kaiser, T. Liu, W. Richtering and A. M. Schmidt, *Langmuir*, 2009, **25**, 7335–7341 doi:10.1021/la900401f.

167 A. L. Fameau, S. Lam, A. Arnould, C. Gaillard, O. D. Velev and A. Saint-Jalmes, *Langmuir*, 2015, **31**, 13501–13510 doi:10.1021/acs.langmuir.5b03660.

168 A. M. Menzel, *J. Chem. Phys.*, 2014, **141**, 194907 doi:10.1063/1.4901275.

169 O. N. Sorokina, A. L. Kovarski, M. A. Lagutina, S. A. Dubrovskii and F. S. Dzheparov, *Appl. Sci.*, 2012, **2**, 342–350 doi:10.3390/app2020342.

170 M. Yu, B. Ju, J. Fu, S. Liu and S. B. Choi, *Ind. Eng. Chem. Res.*, 2014, **53**, 4704–4710 doi:10.1021/ie4040237.

171 K. Lalitha, Y. S. Prasad, V. Sridharan, C. U. Maheswari, G. John and S. Nagarajan, *RSC Adv.*, 2015, **5**, 77589–77594 doi:10.1039/c5ra14744a.

172 M. Tarama, P. Cremer, D. Y. Borin, S. Odenbach, H. Löwen and A. M. Menzel, *Phys. Rev. E - Stat. Nonlinear, Soft Matter Phys.*, 2014, **90**, 42311 doi:10.1103/PhysRevE.90.042311.

173 A. Stoll, M. Mayer, G. J. Monkman and M. Shamonin, *J. Appl. Polym. Sci.*, 2014, **131**, 39793 doi:10.1002/app.39793.

174 J. Chatterjee, Y. Haik and C. J. Chen, *Colloid Polym. Sci.*, 2003, **281**, 892–896 doi:10.1007/s00396-003-0916-z.

175 J. Chatterjee, Y. Haik and C. J. Chen, *J. Appl. Polym. Sci.*, 2004, **91**, 3337–3341 doi:10.1002/app.13545.

176 S. A. Braim, K. M. Shakesheff, B. R. Saunders and C. Alexander, *J. Mater. Chem. B*, 2016, **4**, 962–972 doi:10.1039/c5tb01739d.

177 N. A. Jalili, M. Muscarello and A. K. Gaharwar, *Bioeng. Transl. Med.*, 2016, **1**, 297–305 doi:10.1002/btm2.10034.

178 F. Ridi, M. Bonini and P. Baglioni, *Adv. Colloid Interface Sci.*, 2014, **207**, 3–13 doi:10.1016/j.cis.2013.09.006.

179 A. Zadrail, V. Tokárová and F. Tpánek, *Soft Matter*, 2012, **8**, 1811–1816 doi:10.1039/c1sm06707a.

Soft Matter

180 X. Fan, X. Dong, A. C. Karacakol, H. Xie and M. Sitti, *Proc. Natl. Acad. Sci. U. S. A.*, 2020, **117**, 27916–27926 doi:10.1073/PNAS.2016388117/SUPPL_FILE/PNAS.2016388117.SM06.MOV.

181 M. Sun, C. Tian, L. Mao, X. Meng, X. Shen, B. Hao, X. Wang, H. Xie and L. Zhang, *Adv. Funct. Mater.*, 2022, **32**, 2112508 doi:10.1002/ADFM.202112508.

182 X. Fan, M. Sun, L. Sun, H. Xie, X. Fan, M. Sun, L. Sun and H. Xie, *Adv. Funct. Mater.*, 2020, **30**, 2000138 doi:10.1002/ADFM.202000138.

183 J. Čejková, T. Banno, M. M. Hanczyc and F. Štěpánek, *Artif. Life*, 2017, **23**, 528–549 doi:10.1162/ARTL_A_00243.

184 J. G. Lee, V. Porter, W. A. Shelton and B. Bharti, *Langmuir*, 2018, **34**, 15416–15424 doi:10.1021/acs.langmuir.8b03232.

185 Z. Chen, D. Zhao, B. Liu, G. Nian, X. Li, J. Yin, S. Qu and W. Yang, *Adv. Funct. Mater.*, 2019, **29**, 1–8 doi:10.1002/adfm.201900971.

186 A. Sydney Gladman, E. A. Matsumoto, R. G. Nuzzo, L. Mahadevan and J. A. Lewis, *Nat. Mater.*, 2016, **15**, 413–418 doi:10.1038/nmat4544.

187 Y. Kim, G. A. Parada, S. Liu and X. Zhao, *Sci. Robot.*, 2019, **4**, eaax7329 doi:10.1126/SCIROBOTICS.AAX7329.

188 S. Roh, L. B. Okello, N. Golbasi, J. P. Hankwitz, J. A. C. Liu, J. B. Tracy and O. D. Velev, *Adv. Mater. Technol.*, 2019, **4**, 1800528 doi:10.1002/admt.201800528.

189 Y. Kim and X. Zhao, *Chem. Rev.*, 2022, **122**, 5317–5364 doi:10.1021/acs.chemrev.1c00481.

190 Y. Kim, H. Yuk, R. Zhao, S. A. Chester and X. Zhao, *Nature*, 2018, **558**, 274–279 doi:10.1038/s41586-018-0185-0.

191 C. Li, G. C. Lau, H. Yuan, A. Aggarwal, V. L. Dominguez, S. Liu, H. Sai, L. C. Palmer, N. A. Sather, T. J. Pearson, D. E. Freedman, P. K. Amiri, M. O. de la Cruz and S. I. Stupp, *Sci. Robot.*, 2020, **5**, eabb9822 doi:10.1126/scirobotics.abb9822.

192 M. Yu, B. Ju, J. Fu, S. Liu and S. B. Choi, *Ind. Eng. Chem. Res.*, 2014, **53**, 4704–4710 doi:10.1021/ie4040237.

193 D. Morales, B. Bharti, M. D. Dickey and O. D. Velev, *Small*, 2016, **12**, 2283–2290 doi:10.1002/smll.201600037.

194 J. Yu, D. Jin, K. F. Chan, Q. Wang, K. Yuan and L. Zhang, *Nat. Commun.*, 2019, **10**, 1–12 doi:10.1038/s41467-019-13576-6.

195 J. Li, B. E. F. De Ávila, W. Gao, L. Zhang and J. Wang, *Sci. Robot.*, 2017, **2**, 6431 doi:10.1126/scirobotics.aam6431.

196 S. Kim, F. Qiu, S. Kim, A. Ghanbari, C. Moon, L. Zhang, B. J. Nelson and H. Choi, *Adv. Mater.*, 2013, **25**, 5863–5868 doi:10.1002/adma.201301484.

197 F. Qiu and B. J. Nelson, *Engineering*, 2015, **1**, 021–026 doi:10.15302/J-ENG-2015005.

198 L. Li, Y. Zhu and J. Yang, *Mater. Lett.*, 2018, **210**, 136–138 doi:10.1016/j.matlet.2017.09.015.

Soft Matter

199 H. Ravanbakhsh, G. Bao, Z. Luo, L. G. Mongeau and Y. S. Zhang, *ACS Biomater. Sci. Eng.*, 2021, **7**, 4009–4026 doi:10.1021/acsbiomaterials.0c01158.

200 S. S. Athukoralalage, R. Balu, N. K. Dutta and N. R. Choudhury, *Polymers (Basel).*, 2019, **11**, 898 doi:10.3390/polym11050898.

201 A. H. Williams, S. Roh, A. R. Jacob, S. D. Stoyanov, L. Hsiao and O. D. Velev, *Nat. Commun.*, 2021, **12**, 12:2834 doi:10.1038/s41467-021-23098-9.

202 D. Kokkinis, M. Schaffner and A. R. Studart, *Nat. Commun.*, 2015, **6**, 1–10 doi:10.1038/ncomms9643.

203 M. M. Schmauch, S. R. Mishra, B. A. Evans, O. D. Velev and J. B. Tracy, *ACS Appl. Mater. Interfaces*, 2017, **9**, 11895–11901 doi:10.1021/acsami.7b01209.

204 J. Zhang, Z. Ren, W. Hu, R. H. Soon, I. C. Yasa, Z. Liu and M. Sitti, *Sci. Robot.*, 2021, **6**, 112 doi:10.1126/scirobotics.abf0112.

205 D. Jiao, C. Shi and G. De Schutter, *Mater. Lett.*, 2022, **309**, 131374 doi:10.1016/j.matlet.2021.131374.

206 Z. Varga, G. Filipcsei and M. Zrínyi, *Polymer (Guildf).*, 2006, **47**, 227–233 doi:10.1016/j.polymer.2005.10.139.

207 S. R. Mishra, M. D. Dickey, O. D. Velev and J. B. Tracy, *Nanoscale*, 2016, **8**, 1309–1313 doi:10.1039/c5nr07410j.

208 D. Morales, E. Palleau, M. D. Dickey and O. D. Velev, *Soft Matter*, 2014, **10**, 1337–1348 doi:10.1039/c3sm51921j.

209 E. Palleau, D. Morales, M. D. Dickey and O. D. Velev, *Nat. Commun.*, 2013, **4**, 1–7 doi:10.1038/ncomms3257.

210 S. R. Mishra, M. D. Dickey, O. D. Velev and J. B. Tracy, *Nanoscale*, 2016, **8**, 1309–1313 doi:10.1039/c5nr07410j.

211 M. Tarama, P. Cremer, D. Y. Borin, S. Odenbach, H. Löwen and A. M. Menzel, *Phys. Rev. E - Stat. Nonlinear, Soft Matter Phys.*, 2014, **90**, 042311 doi:10.1103/PhysRevE.90.042311.

212 H. N. An, B. Sun, S. J. Picken and E. Mendes, *J. Phys. Chem. B*, 2012, **116**, 4702–4711 doi:10.1021/jp301482a.

213 Y. Wang, Y. Zhang, Y. Guan and Y. Zhang, *Langmuir*, 2022, **38**, 6057–6065 doi:10.1021/acs.langmuir.2c00297.

214 Y. Guo, J. Zhang, W. Hu, M. T. A. Khan and M. Sitti, *Nat. Commun.*, 2021, **12**, 1–9 doi:10.1038/s41467-021-26136-8.

215. R. Sharma, S.-T. Chang and O. D. Velev, Langmuir, 2012, **28**, 10128−10135. DOI: 10.1021/la301437f

216. J. Deng, M. Molaei, N. G. Chisholm, T. Yao, A. Read, K. J. Stebe, *Curr. Opinion Colloid Interface Sci.,* 2022, **61**, 101629, doi.org/10.1016/j.cocis.2022.101629**.**